DIFFERENTIAL GENE EXPRESSION IN THE SKIN OF *XIPHOPHORUS MACULATUS* JP 163 B IN RESPONSE TO FULL SPECTRUM (10,000 K) FLUORESCENT LIGHT

by

Kaela Caballero, B.S.

A thesis submitted to the Graduate Council of
Texas State University in partial fulfillment
of the requirements for the degree of
Master of Science
with a Major in Biochemistry
August 2015

Committee Members:

Ronald Walter, Chair

Rachell Booth

Steven Whitten

FAIR USE AND AUTHOR'S PERMISSION STATEMENT

Fair Use

Duplication Permission

DEDICATION

To my parents and family, who have always supported and encouraged me, my education and my coffee addiction. And to Max, my study buddy; where you have gone, there is no need for coffee fueled late nights. Rest in peace.

ACKNOWLEDGEMENTS

This work could not have been accomplished without the support and mentorship that I have received throughout my life from family, teachers, mentors and friends. It is impossible to name everyone here, but I would like to use a few lines to thank those that have helped me achieve my goals.

Thank you to Dr. Ron Walter for your support and mentorship this last year and half. It has definitely been a journey; you have pushed me to be better in all aspects of my life and have put up with me when I failed. My gratitude towards you cannot be adequately expressed, so I hope that through my continued success I can convey the appreciation I have for the opportunities and lessons you have allowed me to take part in. I hope that one-day I can show you that the time and support you have shown me where well spent. I would also like to thank the various current and former members of the Molecular Biosciences Research Group and *Xiphophorus* Stock Center Staff: Will and Mikki Boswell, Markita Savage and Natalie Taylor, and graduate students Jordan Chang and Angelica Riojas for their help, support and fellowship during my time here.

Thank you to UTHSCSA coordinators of the Doctoral Bridge program, Dr. Nicquet Blake and Dr. Kay Oyajobi, for your continuous support and guidance from the time I applied to Texas State and throughout my time here. Thank you to my committee members Dr. Rachell Booth and Dr. Steve Whitten for your academic input and mentorship during my time here. It has been greatly appreciated and invaluable.

Lastly, to my parents, fiancé, family and friends: to give thanks for your continuous love, support, understanding and sacrifice is not even minimally adequate. I could not have made it this far without your love and encouragement. Thank you.

TABLE OF CONTENTS

Page

LIST OF TABLES

Table **Page**

LIST OF FIGURES

Figure **Page**

ABSTRACT

Over the past decade physiological and psychological effects of artificial fluorescent lighting on humans has been shown to be significant and quantifiable. Both the amount and composition of lighting are important parameters associated with human and animal health. Published reports suggest human physiological responses to "full spectrum" vs. "cool white" lamps include differences in oxygen intake, heart rate, absorption of vitamins and minerals, etc. Despite many behavioral and physiological studies indicating artificial light sources may be important to health there exists a paucity of data regarding specific molecular genetic responses occurring in tissues of intact animals upon exposure to varying types of artificial lighting.

Tropical fishes, such as *Xiphophorus*, may be expected to represent vertebrate experimental models that are both very sensitive and responsive to varying light conditions. In the wild, fishes utilize light conditions for warmth, predation, predator avoidance, and to coordinate breeding cycles. Recently, our laboratory has been employing *Xiphophorus* fishes and RNA-Seq methods to investigate global changes in skin gene expression after exposure of the intact animal to various types of lighting and wavelengths. This was initiated as a means to identify genetic patterns that may hallmark a predisposition to melanoma induction, but comparison of data indicated fluorescent light exposure resulted in a molecular genetic response nearly as great in amplitude as observed for ultraviolet B (UVB) exposure. Given the current widespread use of fluorescent lighting in human and animal facilities, we sought to examine the extent other

light sources may influence molecular genetic regulation in fish skin. Herein, we present results showing exposure to full spectrum fluorescent light (10,000 K) affects different biological processes in *Xiphophorus* skin.

Biological replicates of *Xiphophorus* males Jp 163 B were exposed to varying doses of 10,000 K light. Functional pathway analyses revealed an overall shared suppression of expressed genes associated with cell cycle phase transition, mitotic spindle assembly, chromosome segregation and DNA replication, while shared genes increased in expression were associated with the circadian-rhythmic process and cell structure. Unique responses were observed at individual exposures, the majority of which were represented by genes exhibiting an increase in expression. These unique responses were associated with lipid and cholesterol catabolism, phosphorylation and epidermis structure. Our results suggest exposure to full spectrum fluorescent light largely results in stalling of mitotic progression, induces catabolic processes and implicates inflammatory response in skin. Overall, these results characterize the genetic responses induced by 10,000 K light in *X. maculatus* Jp 163 B skin.

CHAPTER I

INTRODUCTION

Fish Models in Research

Teleost fish (i.e., ray-finned fishes) models have contributed to the understanding of a variety of biomedical and biological topics spanning subjects such as developmental biology, toxicology, physiology, comparative genetics and tumorigenesis (Walter and Kazianis, 2001; Bofellii *et al*, 2004; Patton *et al*, 2010). Fish experimental models have proven useful in research due to their extreme biological diversity, documented genetic synteny, high fecundity, and relatively low cost that allows investigations to achieve statistical power (Patton *et al*., 2010). However, the true power of teleost models for biomedical applications is derived from their phylogenetic status as vertebrates. Despite an estimated divergence time of about 360-450 million years ago (Volf, 2005), teleosts and land vertebrates are similar in their comparative anatomy (Diogo *et al*, 2008), embryonic development (Gilbert, 2000) and genomics (Aparicio *et al*, 2002; Woolfe *et al*, 2005). Teleosts share approximately the same functional set of genes as mammals**,** but generally have a fraction of the genome size (Hedges and Kumar, 2002). Sequenced teleost genomes have been useful in identifying functional regions of genes in their mammalian counterparts (Aparicio *et al*, 2002; Boffelli *et al*, 2004; Woolfe *et al*, 2005). Herein we utilize *Xiphophorus*, a new world order of live bearing teleost fishes. *Xiphophorus* fishes have been used as a vertebrate model to study genetic inheritance underlying tumorigenesis for over 85 years (Gordon, 1931; Schartl *et al*, 1995; Nairn *et al*, 1996; Weis and Schartl, 1998; Mitchell *et al*, 2010; Schartl *et al*, 2013).

Xiphophorus Fishes

The *Xiphophorus* genus encompasses 26 species of viviparous (i.e., live-bearing) tropical freshwater fishes whose natural range includes Mexico and southward to Belize and Honduras in Central America (Kallman and Kazianis, 2006). Pedigreed lines of *Xiphophorus* are maintained at the *Xiphophorus* Genetic Stock Center in San Marcos, TX, USA (www.xiphophorus.org) and these are made available to researchers worldwide. Of the current pedigreed species, there are lines in their 113th (*X. maculatus* Jp 163 A) and 106th (*X. maculatus* Jp 163 B) generation of sister-brother inbreeding. Such inbreeding is expected to maintain the fish line in an essentially homozygous state (Russell, 1941; Poiley, 1975). The complete genome for one such pedigreed fish, *X. maculatus* Jp 163 A, has been sequenced, assembled, and is publically available (Schartl *et al*, 2013; http://www.ensembl.org/Xiphophorus_maculatus/Info/Index). This genome and its annotations have been useful in profiling global genetic expression (i.e. RNA-seq) in various tissues when employing *Xiphophorus* in a variety of research investigations.

Xiphophorus as a Model to Study Inherited Tumorigenesis

The most well studied *Xiphophorus* interspecies hybrid cross (Gordon, 1931) is between *Xiphophorus maculatus* Jp 163 A (a Southern platyfish) and *X. helleri* (a swordtail) with the F_1 hybrid backcrossed to the swordtail parental line (Fig. 1-1). In this cross, termed the Gordon-Kosswig (or G-K) model, the *X. maculatus* Jp 163 A carries the spot dorsal (*Sd*) pigment pattern (i.e., black pigmentation; Anders, 1967) on the dorsal fin while the *X. hellerii* parent does not. This phenotype is derived from melanin expression in special types of skin cells termed macromelanophores (Gordon, 1927; Vielkind and Vielkind, 1982). First generation G-K interspecies hybrids (F_1 hybrids) exhibit an

enhanced pigmentation pattern of the dorsal fin, compared to either parent. This enhancement is thought to be due to loss of a one copy of the autosomal locus *Diff*, that serves to keep expansion of the *Sd* pigment pattern in check within the *X. maculatus* parent (Vielkind, 1976). Thus, the *Diff* locus (also known as *R*, for regulator; Meierjohann and Schartl, 2006) is thought to functionally control differentiation of *X. maculatus* macromelanophores (Anders, 1967; Vielkind *et al*, 1989).

In the G-K cross, backcross of the F_1 offspring to the *X. helleri* parental species produce progeny (BC_1) that exhibit a 1:1 genotypic distribution of both the *Sd* and *Diff* loci (Anders, 1967; Vielkind *et al*, 1976). Thus, 50% of the BC_1 progeny inherit the *X. maculatus Sd* pigment pattern. Of these pigmented animals 50% (25% of the total BC_1 offspring) express enhanced pigmentation in the dorsal fin resembling the F_1 hybrids, while, 50% express very heavy pigmentation in the dorsal fin that expands as the fish ages along the dorsal flanks and posterior of the animal. The pigment expansion in the BC_1 fish with heavy pigmentation is melanoma, (i.e. uncontrolled proliferation of melanin containing cells) derived from macromelanophores, that invade the musculature and result in necrosis of the dorsal fin and surrounding tissue base, eventually resulting in mortality (Walter and Kazianis, 2001). Formation of melanoma is due to a gene (*Tu*) that is linked to the *Sd* pigment pattern locus on the X chromosome (Nairn *et al*, 1996). *Tu* is an oncogene (i.e. a gene that promotes rapid and uncontrolled proliferation of cells) regulated by presence of the theoretical *Diff* tumor suppressor locus in *X. maculatus* (Adam *et al*, 1993; Kazianis *et al*, 1998, Meierjohann and Schartl, 2006).

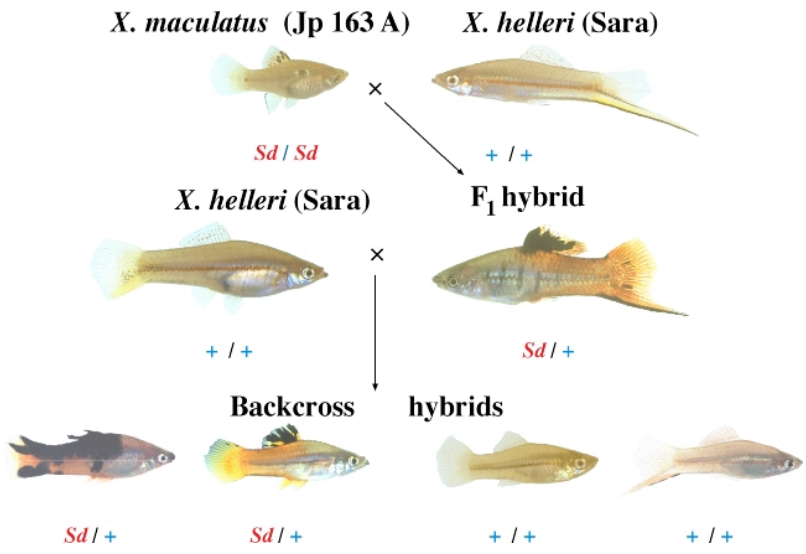

Fig. 1-1: The Gordon-Kosswig model in *Xiphophorus* hybrids. *X. maculatus* Jp 163 A is a homozygous carrier of *Sd*. *X. maculatus* is crossed with *X. helleri* to produce F_1 hybrids that exhibit enhanced dorsal fin pigmentation, believed to be due to loss of a *Sd* regulator, *Diff*. F_1 hybrids backcrossed to the *X. helleri* parent produce offspring with ranging in degree of pigmentation.

Source: http://www.xiphophorus.txstate.edu/stockcenter/galleries/hybrid.html

Xiphophorus interspecies crosses have also been developed that do not lead directly to tumor formation in BC_1 hybrids, but produce animals exhibiting tumor inducibility after exposure to DNA damaging agents (Kazianis *et al*, 2001a,b). For example, the cross of *X. maculatus* Jp 163 B, carrying the spot side (*Sp*) pigment pattern, with *X. couchianus* leads to F_1 animals exhibiting enhanced pigmentation on the flanks from pectoral to the tail fin (Kazianis *et al*, 2001a). These F_1 hybrids, when backcrossed to the *X. couchianus* parental line, show a range of pigmentation, as in the G-K cross, from non-pigmented (50%), to mottled full body pigmentation like the F_1 (25%) to very heavy pigmentation being nearly black from head to tail (25%). However, in this cross melanoma tumors develop if the pigmented BC_1 offspring are exposed to *N*-nitroso-*N*-methylurea (MNU; 6 weeks post-birth) or ultraviolet-B light (UVB; 6 days post birth;

Kazianis *et al*, 2001a,b, Walter and Kazianis, 2001). These induced melanomas occur as nodular lesions that expand with time and can become quite large.

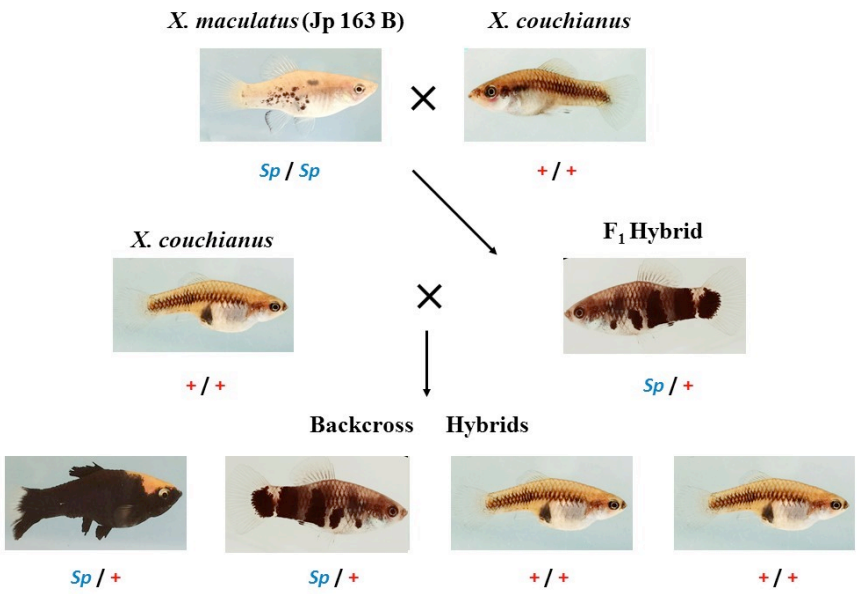

Fig. 1-2: *Xiphophorus* inducible melanoma cross. *X. maculatus* (Jp 163 B) is crossed with *X. couchianus*. The F1, and 50% of the BC_1 hybrids of this cross have enhanced pigmentation along their side flanks, derived from partial regulation of Tu.

Source: Angelica Riojas

Contribution of Ultraviolet Radiation to Formation of Melanoma in *Xiphophorus*

As discussed above, ultraviolet (UV) light can be used to induce melanoma in certain *Xiphophorus* hybrids. In humans, increased incidence of skin cancers, including melanoma, is associated with extended exposure to sunlight. This is widely believed to be due to the UV wavelengths present in sunlight (Armstrong *et al*, 1997; Jemal *et al*, 2006). UV light is comprised of wavelengths that range from 280-400 nm (Wenk *et al*, 2001). There are three classes of UV light: UVA (320-400 nm), UVB (280-320 nm), and UVC (240-280 nm) (Wenk *et al*, 2001). UVC and the majority of UVB waves are prevented from reaching the Earth's surface due to atmospheric filtration by ozone (Maverakis *et al*,

2010). Thus, UVA waves make up the majority (~95%) of UV light that reaches the Earth's surface (Maverakis *et al*, 2010). *Xiphophorus* hybrids that exhibit UV inducible tumor development have been useful in trying to characterize the precise UV wavelengths that lead to melanoma induction.

UVA has primarily been thought to contribute to melanoma formation through oxidation of melanin in melanocytes (Wood *et al*, 2006). Exposure of melanin to UVA results in a generation of surplus radical oxygen species (ROS) (e.g. superoxide anion, ($O_2^{\bullet -}$), hydroxyl radicals ($OH^{\bullet}$), singlet oxygen ($^1O_2$), and hydrogen peroxide (H_2O_2)). ROS are common by-products of cellular metabolic processes (Loschen and Flohe, 1992; Boveris and Chance, 1973) that have the ability to modify DNA bases, lipids and proteins through oxidative reactions (Aruoma, 1999; Mitchell *et al,* 2007). Normally, cellular levels of ROS are regulated by a variety of antioxidant radical scavenging molecules or enzymes, such as superoxide dismutase or glutathione-S-transferase, (Wenk *et al*, 2001). However, in cells directly exposed to UVA the balance of ROS to antioxidants is shifted towards a surplus of ROS, resulting in oxidative stress and an increase in oxidative damage to DNA bases (Zhang *et al*, 1997a,b). Setlow *et al*. (1993) characterized the action spectrum for melanoma tumor induction in *Xiphophorus* backcross hybrids. In this study hybrids exposed to UVA wavelengths of 365 or 405 nm (UVA region) exhibited tumors four months after exposure (Setlow *et al*, 1993). Wood *et al*. (2006) characterized the action spectrum of ROS generation in *Xiphophorus* exposed to light in the 300-440 nm range. The rate at which UV induced generation of ROS (i.e. action spectrum) coincided with that of melanoma induction, supporting the idea that ROS contribute significantly to melanoma formation (Wood *et al*, 2006).

Whereas UVA exposure cause cellular damage indirectly via oxidative reactions via cellular photosensitizers (i.e., melanin), UVB can directly damage DNA (Rastogi *et al*, 2010). This is due to strong absorption of UVB by pyrimidine bases (i.e. cytosine or thymine) that, if adjacent to another pyrimidine, can result in the formation of cyclobutane pyrimidine dimers (CPDs), 6-4 photoproducts (6-4 PPs), or their Dewar isomers (Rastogi *et al*, 2010). Pyrimidine dimers have also been associated with tumor formation in UVB exposed *Poecilia formosa* (Hart *et al.*, 1977) and in melanoma formation of *Xiphophorus* hybrids (Mitchell *et al*, 2001, 2007). While it is evident both UVA and UVB cause damage to melanin containing cells, the amount of photodamage is not only dependent on the amount of UV a cell receives, but also the ability of an organism to repair UV induced damage (Maverakis *et al*, 2010).

Photoreactivation

In vertebrates, including humans, CPDs and 6-4 PPs are removed from DNA by nucleotide excision repair (NER) (Mitchell and Nairn, 1989; Li *et al*, 2010). Most vertebrates (Hart *et al*, 1977; Ley, 1985; Ahmed and Setlow, 1993; Uchida *et al*, 1997; Meador *et al*, 2000; Mitchell *et al*, 2001; Armstrong *et al*, 2002), prokaryotic organisms (Kelner, 1948) and plants (Chaves *et al*, 2011) also have the ability to utilize visible light to restore UV induced CPDs and 6-4 PPs to monomer bases via a process termed photoreactivation. Essential to photoreactivation are DNA repair enzymes termed photolyases (CPD and 6-4 photolyase) that use light from the visible light range (320-500 nm) to break apart UV induced dimerization (Sancar, 2003).

The mechanism for CPD photolyase is currently better defined than that of 6-4 photolyase. CPD photolyases have two distinct light sensitive moieties, a chromophore

that absorbs photons from light in the visible light spectrum (350-450 nm) (Sancar, 2003), and a second chromophore that uses a tunneling pathway to channel energy from captured photons to split the cyclobutane bonds, thus restoring the dimerized bases to their monomer states (Liu *et al*, 2011; reviewed by Walter *et al.*, 2014). Comparatively, the 6-4 photolyase is thought to repair 6-4 photoproducts via a mechanism that utilizes cyclic proton transfer between the enzyme and the 6-4 photoproduct (Li *et al*, 2010). Photolyases have been shown to be active in cultured cells of *C. auratus* (goldfish) (Uchida *et al,* 1997), *Xenopus* (clawed frog) (Griggs and Bender, 1972), *P. tridactylis* (rat-kangaroo) (Krishan and Painter, 1973), as well as intact vertebrates such as *M. domestica* (a short-tailed opossum) (Ley, 1985), *P. formosa* (Amazon molly) (Hart *et al*, 1977), *O. latipes* (medaka) (Armstrong *et al*, 2002), and *Xiphophorus* fishes (Ahmed and Setlow, 1993; Meador *et al*, 2000; Mitchell *et al*, 2001; Walter et al., 2014).

Evidence for a Specific Response to Fluorescent Light

In a laboratory setting, photoreactivation can be induced with "white" fluorescent light (Setlow *et al*, 1989 Uchida *et al*, 1997; Meador *et al*, 2000). White light is generally used to describe the color of light created from a combination of other colors (Sheehan, 2009). Fluorescent light, common in many businesses, buildings, and homes is produced when a small amount of mercury within a vacuum lamp tube is vaporized by electric energy (Meyer *et al*, 1939). The vaporization of mercury requires absorption of energy, in this instance heat, which causes the mercury atoms to transition to a higher energy state (Srivastave and Ronda, 2004). Mercury vapor atoms emit ultraviolet light of ~250 nm (Srivastave and Ronda, 2004), which is converted to visible light through interaction with fluorescent materials (i.e. phosphors) (Smets, 1987) that coat the inside of the lamp. The

precise wavelengths of light produced by fluorescent lamps is dependent on the combination of phosphors used and varies in perceived color (Srivastave and Ronda, 2004).

"Cool white", "daylight" and "full spectrum" are terms that have been loosely used to describe different types of fluorescent lights (Bielski *et al*, 1992). Cool white is generally associated with fluorescent lights that have a large region of wavelengths in the blue-green (495 nm) and yellow (575 nm) regions (Thronton, 1971; Bielski *et al*, 1992), while, full spectrum has been used to describe light that simulates the full spectrum of the sun (Bielski *et al*, 1992) (**Fig. 1-3**). The colors emitted by different types of fluorescent lights are defined by a Kelvin correlated value (Lucero-Vera *et al.*, 2009). These values are established by heating a theoretical black body radiator to a color matching that of the fluorescent light. The temperature, measured in Kelvin, is assigned to that particular fluorescent light color (Lucero-Vera *et al.*, 2009).

Human health reports have suggested there may be differences between "cool white" versus "full spectrum" fluorescent light (McColl and Veitch, 2001) that could differentially affect human heart rate (Chance, 1983), oxygen intake (Chance, 1983), and hormone levels (Kuller and Lindsten, 1992).

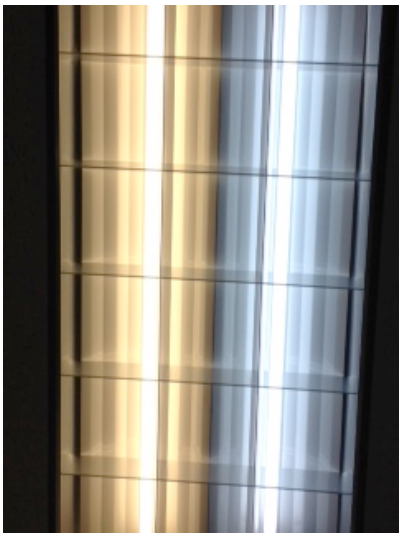

Fig. 1-3: A side by side visual comparison of "cool white" (left) and "full spectrum" lights (right).

Source: Dr. Ronald Walter

Xiphophorus fishes provide an excellent biological model in which to study the effects of light on the intact vertebrate organism. As discussed earlier, Setlow *et al.* (1989) reported tumor induction in *Xiphophorus* backcross hybrids exposed to UV light. However, in the same study subsequent exposure to cool white fluorescent light after the UV treatment reduced tumor prevalence in the backcross hybrids most susceptible to melanoma formation (Setlow *et al.*, 1989). The observed reduction in tumor prevalence after the additional fluorescent light exposure suggests fluorescent light may induce a photoreactivation response in *Xiphorphous* antagonistic to the effects of UV.

Separate RNA-Seq studies investigating the molecular genetic response to different light sources (i.e. UVB and cool white fluorescent) have been performed using *Xiphophorus*. Yang *et al*. (2014) observed a dose dependent expression of genes involved in protein activation, inflammation, and the immune response within fish skin exposed to UVB (311 nm). In unpublished work within our laboratory, RNA-Seq studies of *X.*

maculatus males exposed to varying doses of cool white fluorescent (4,100 K) light have revealed altered expression in sets of genes associated with cell cycle progression, mitosis, DNA repair, and DNA replication in skin (Walter, R.B., unpublished). Collectively, these studies indicate there are unique molecular genetic responses that occur in the skin of intact *Xiphophorus* upon exposure to varying sources of light. Thus, characterization of global genetic responses to various light sources may assist our understanding of genes and pathways involved in induced melanoma development, and further, may identify primary genetic effects that different light sources may induce in vertebrates, perhaps including humans.

The current study was focused on investigation of the global genetic changes brought about in *Xiphophorus maculatus* Jp 163 B skin after exposure to full spectrum fluorescent (10,000 K) light. We employed RNA-Seq methodology combined with bioinformatic data-mining to identify shifts in gene expression after 10,000 K light exposure. We present results of gene expression profiling in skin after various doses of 10,000 K light, report clusters of shared genes and functions and show a molecular genetic response of shared response among increasing doses of 10,000 K exposure. The findings of this study increase our understanding of the molecular genetic response to specific sources of light in the skin of intact male *X. maculatus,* provide comparative data for other light sources, and forward our knowledge of the dynamic nature of organismal adaption to external stimuli.

CHAPTER II

METHODS & MATERIALS

Research Animals

All *Xiphophorus maculatus* Jp 163 B utilized in this study were maintained in 5 to 20 gallon freshwater aquaria and fed twice daily, either newly hatched brine shrimp (*Artemia*) nauplii and beef liver paste (Gordon, 1943b). The pedigreed fish used in this study were all mature adult males, 12 months in age, obtained from the *Xiphophorus* Genetic Stock Center (Texas State University, San Marcos, TX; http://www.xiphophorus.txstate.edu/).

X. maculatus Jp 163 B (pedigree 104 D) (**Fig. 2-1**) were derived from one single field-inseminated female fish in 1939 from the Rio Jamapa (Veracruz, Mexico). The offspring were split after approximately nine generations of sibling-sibling inbreeding to generate the pedigrees Jp 163 A and Jp 163 B. *X. maculatus* Jp 163 B used in this study are of the 104th generation.

X. maculatus Jp 163 B 104d

Fig. 2-1: Image of X. maculatus Jp 163 B used in this study.
Source: Kaela Caballero

Light Sources and Exposures

Full spectrum light (10,000 K) exposures were carried out in a specially designed wooden box (77 cm in length, 41 cm in height, and 36 cm in depth), with a hinged wooden lid capable of sealing the interior of the box from external light (Fig. 2-2). On the bottom of each of the two sides (41 cm x 36 cm) were 15.5 cm diameter high-speed fans that maintained interior temperatures of the closed box at less than 24°C. For full spectrum exposures single fish were placed into UV transparent (UVT) plastic cuvettes (9 cm x 7.5 cm x 1.5 cm) in about 95 mL of filtered aquarium water. The cuvettes were suspended in a rack centered between and about 10 cm between four Coralite T8 17W 10,000K "daylight" (full spectrum; herein termed CO) lamps, configured with two lamps mounted on each side of the interior of the exposure chamber. Fluence (i.e., radiant power) was measured on each side of the chamber using a Newport Power Meter (International Light, Newburyport, MA, model 1918-R). The average fluence for the 10,000 K full spectrum lamps was 14.2 J/ m^2. The spectral distribution was measured with an Ocean Optics Spectrometer (**Fig. 2-3**; Spectrecology, Jasper, GA, model USB4000-FL)

All animals were placed in the dark at 6:00 pm the day before experimental exposures, individually in 125 mL flasks filled with 100 mL of filtered aquaria water. After CO exposure the following morning, fish were maintained in the dark for 6 hrs to allow time for gene expression prior to sacrifice and tissue dissection. At dissection fish were sacrificed by cranial pith after anesthesia in an ice water bath. Skin, as well as other organs, were dissected directly into RNAlater (Ambion Inc., Austin, TX, AM7021), frozen, and stored at -80°C.

Fig. 2-2: Images of the exterior (top) and interior (bottom) of the exposure box used for light exposures. Two fish at a time were exposed in individual 9 cm (length) x 7.5 cm (height) x 1.5 cm (width) UV-transparent chambers suspended between two banks of Coralite T8 17W 10,000 K “daylight” (bottom panel) lamps mounted horizontally on each side of the chamber.

Source: Kaela Caballero

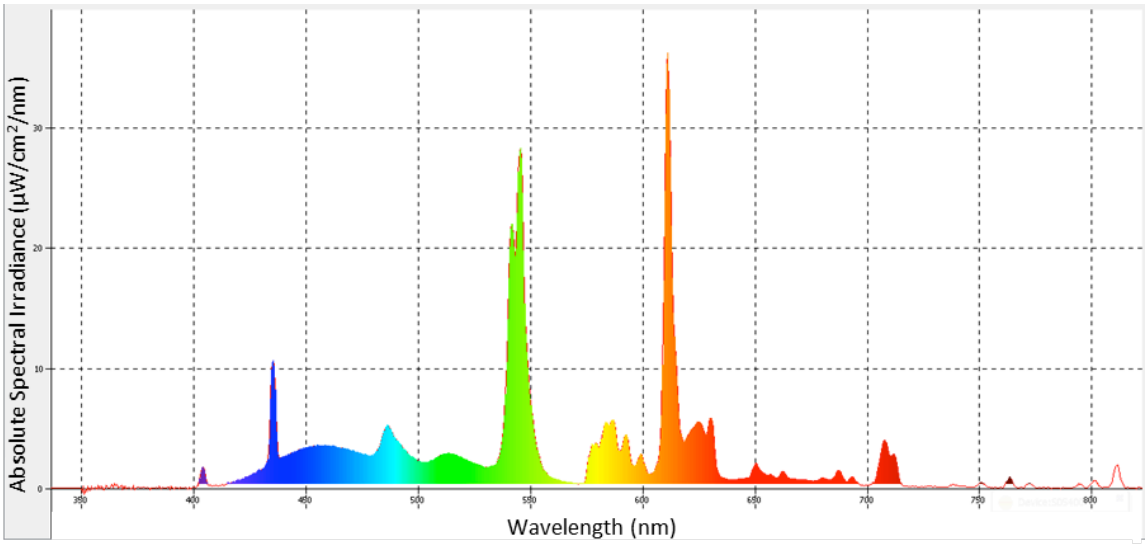

Fig. 2-3: Spectral distribution of the four Coralite T8 17W 10,000K "daylight" (full spectrum; CO) lamps. Distribution was measured

Source: William Boswell

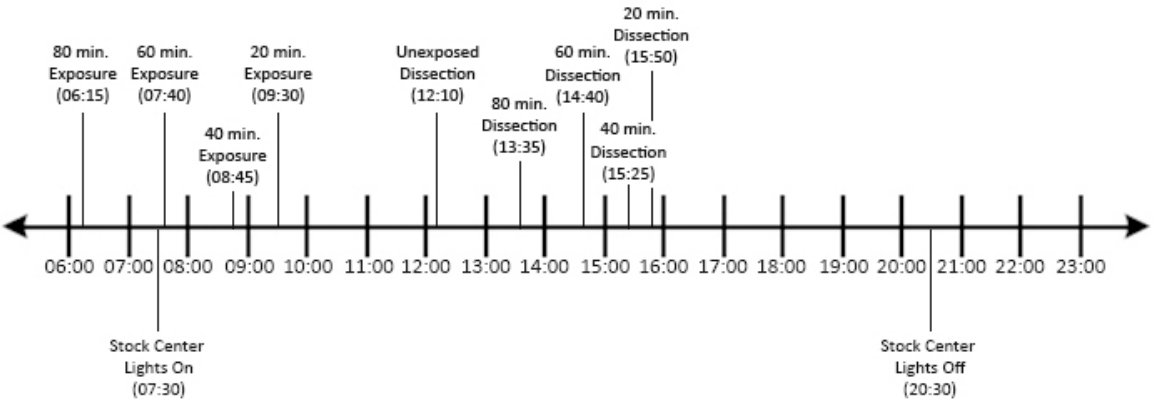

Fig. 2-4: Timeline depicting hours fish are normally exposed to light, hours of experimental exposure to CO and dissection times. Fish were placed in the dark at 6 PM the night before experimental exposures were conducted.

RNA Isolation

After dissection flash frozen skin samples were macerated manually in a total of 0.6 mL of TRI reagent (Sigma-Aldrich, St. Louis, MO, Product #: 93289), followed by mechanical disruption with a pestle and Dremel tool (http://www.dremel.com). Following homogenization, samples were incubated at room temperature for 5 min followed by the addition of 0.12 mL chloroform. Samples were vigorously shaken then centrifuged at 12,000 x g for 5 min at 4°C. A second TRI reagent-chloroform extraction was performed on the extracted aqueous phase with the addition of 0.3 mL TRI reagent and 0.06 mL of chloroform.

Nucleic acids were precipitated from the extracted aqueous phase with addition of one volume of 70% ethanol. RNA was further purified using an RNeasy minispin RNA isolation kit (Qiagen, Valencia, CA). Any residual DNA was eliminated by performing a DNase digestion at 37°C (15 min) on the minispin column. RNA was quantified using a Qubit 2.0 fluorometer (Life Technologies, Grand Island, NY, USA). Prior to High-Throughput Illumina sequencing the integrity and concentration of RNA was assessed employing a BioAnalyzer (Agilent, Santa Clara, CA). The BioAnalyzer generates an RNA Integrity Number (RIN) based on integrity of an RNA sample. Samples with RIN scores below 8 were not used for Illumina sequencing.

RNA Sequencing

X. maculatus Jp 163 B skin biological replicate RNAs were independently sequenced using the Illumina High-Seq platform (75 bps, paired-end (PE) reads) at the MD Anderson Cancer Research Facility (Austin, TX). About 53-98 million raw 75 bp PE reads were generated for each sample. Raw reads were filtered and trimmed based on quality scores using a custom filtration algorithm that removed low-scoring sections of each read and preserved the longest remaining fragment (Garcia *et al.*, 2012). All raw reads were subsequently truncated by similarity to library adaptor sequences using a custom Perl script. Overlapping PE reads were merged using FLASH (Magoc and Salzberg, 2011). Detailed statistics on raw and filtered reads are shown in **Table 2-1**.

Table 2-1: Table showing read statistics for each skin sample. Biological duplicates are differentiated by 'A' and 'B'. X = average number of times each nucleotide is expected to be sequenced given a certain number of reads of a given length and the assumption that reads are randomly distributed across an idealized genome (Landers *et al.*, 2001).

Exposure (min)	Reads Mapped (M)	Reads Unmapped (M)	% Mapped	Average Coverage (X)
0-A	30	23	57.4	66
0-B	41	30	57.7	67
20-A	57	41	58.7	93
20-B	45	31	58.8	73
40-A	47	36	56.4	76
40-B	52	37	58.6	85
60-A	41	29	58.2	67
60-B	45	32	58.5	74
80-A	49	35	58.0	79
80-B	47	32	58.9	76

Filtration and Read Mapping

All filtered reads were mapped to the *X. maculatus* reference transcriptome (Ensembl v78) using the Genomic Short-read Nucleotide Alignment Program (GSNAP) (Wu and Nacu, 2010). Read mapping statistics were calculated using the script Samtools flagstat. The percentage of mapped reads was calculated by dividing the number of mapped reads by the number of filtered reads, then multiplying by 100. Nucleotide coverage was determined by multiplying the number of reads mapped by the length of a read (75 bp) and dividing by the length of the transcriptome (45,942,023 bases).

The DESeq package (v1.18.0, Bioconductor v 2.6, R v2.11) is specifically tailored for work with short-read RNA-Seq data. DESeq was utilized to determine differential gene expression from the mapped transcriptome data (Anders and Huber, 2010). DESeq uses a negative binomial distribution to determine the significance of modulation in gene expression. Genes were considered significant if: genes met a p-adj $\leq$ 0.05 (used in the establishment of control genes in the unexposed samples) or a level of p-adj ≤ 0.01 (used for all exposed samples), and if they met a cutoff of ±2 of the fold change, which was calculated based on comparison of the number of normalized reads within the unexposed skin samples relative to each exposed sample.

Functional Analysis

Interacting genes may be expected to show nonrandom patterns in cell localization, molecular function, and/or biological process thus, bioinformatics analysis on exposure data was performed using DAVID Gene Ontology (Huang *et al.*, 2008). Significant differentially expressed genes (p-adj. < 0.01, ±2 fold change) in each gene set were clustered into gene ontologies using DAVID Gene Ontology

(http://david.abcc.ncifcrf.gov, Huang et al., 2009). DAVID provides gene-annotation enrichment analysis in addition to functional annotation clustering of large gene sets. Gene ontologies (GOs) with an enriched *p*-value greater than 0.01 were not considered. Redundant GOs were consolidated using REViGO (http://revigo.irb.hr/, Supek *et al.*, 2011), a program which summarizes extensive GO lists. Remaining GOs were further consolidated if all genes within the category were found within a larger ontology.

The remaining unique genes were then used to visualize interactions and associations in GeneMania (www.genemania.org, Warde-Farley *et al*., 2010). GeneMania is a gene networking software that was used to visualize physical interactions of protein products, genetic interactions and shared protein domains through a series of lines connecting nodes. Nodes are differentially colored to designate between queried (black) and predicted (grey) genes. Both nodes and lines have a thickness and length that is primarily based on how well connected genes are with each other as reported in publicly available databases. Thicker lines indicate stronger associations.

Quantitative Real Time PCR

Total RNA was isolated from two independent biological replicates of highly inbred *X. maculatus* Jp 163 B males. Isolated RNA was used in cDNA synthesis employing a High Capacity cDNA reverse transcription kit (Applied Bioscience, Carlsbad, CA). Reverse transcription was performed by adding 1.5 µg RNA, 100 mM dNTPs, 10X RT random primers, RNase inhibitor, and MultiScribe Reverse Transcriptase (50u/µL) in a 20 µL reaction employing standard thermocycler conditions (25°C for 10 min, 37°C for 120 min and 85°C for 5 min). Negative controls were synthesized without the reverse transcriptase. Each sample was diluted to a final volume

of 500 µL with 0.1 % DEPC treated water. Expression of select genes was analyzed via qRT-PCR utilizing SYBR Green-based detection on an Applied Biosystems 7500Fast system (Applied Bioscience, Carlsbad, CA).

PCR primers were designed using Geneious (Biomatters Ltd, Auckland, New Zealand) bioinformatic software. All primers were designed with T_m between 60 and 62°C in 3.0 mM K^+, 50 mM Na^+, and 0.8 mM dNTPs with a maximum difference of 1°C between T_ms for each primer in a set. Primer lengths were limited to 18-26 bp in length with 40-60% GC content. Additionally, all amplicons were limited to 70-150 bp in length and were designed to cross at least one exon junction. Primers meeting these criteria and specific for the *Xiphophorus* genes validated are given in **Table 2-2**. Initially, the efficiency of each set of designed primers was tested in triplicate in a 20 µL reaction consisting of a standard serial dilution series of 100, 10, 1, 0.1 ng cDNA, 0.5 µM of each primer, and 10 µL SYBR Green ready mix (Applied Bioscience, Carlsbad CA). Each reaction was subjected to 40 cycles each at 95°C for 20 sec, 95°C for 15 sec, and 60°C for 30 sec, before being subjected to melting curve analysis.

The 18S RNA was selected as the transcript for normalization of all samples. Only primers with efficiencies between 70 and 120% were selected for further use. Once the efficiency and specificity were established, the primers were used to test relative expression of each gene from cDNAs (12 ng) produced from each skin sample.

The threshold cycle (C_T) for each test target and 18S rRNA control was determined by the 7500 Fast System SDS 2.0.6. The average 18S control C_T was subtracted from the average target C_T for each biological replicate independently over 2 biological replicates to give a ΔC_T value. Expression was then determined relative to the

18S rRNA endogenous control by applying $2^{-\Delta CT}$. This represents the mRNA expression level for each target tested relative to the 18S rRNA control. Fold changes for samples exposed to CO were determined relative to each respective basal level tissue ($\Delta\Delta C_T$) (Schmittgen and Livak, 2008). Standard deviations were calculated for the average of 4 technical replicates from each biological replicate.

Table 2-2: Primer sequences for select genes used in quantitative-real time PCR validation of a select subset of significant DE genes.

Gene Name	Ensembl ID	Forward Primer Sequence (5'-3')	Reverse Primer Sequence (3'-5')
cenp-f	ENSXMAT00000015178	GCGTCTGAAAA GAGCCCTG	CCTCCTCCTCA TTGATCATCTCC
cpd	ENSXMAT00000004764	CTCTCAGCCAG CTCTCCC	ACCAGCTCCTC GATGAAGG
igf1ra	ENSXMAT00000003758	CAAAGCCCGTC ATGCCTAAC	GCATAAGTGTG TGTCGCATCAG
per1b	ENSXMAT00000015376	TGCTCTCAAAT ACGCCCTGC	CAGCCATGACA CTCCTCCAC
pold2	ENSXMAT00000015408	GGTCTCCAATC CATACGAAGCC	GGCTGTCCATG CTGCTGTAC
sptbn4	ENSXMAT00000006073	TCACGCTCGGC CTTATCTG	CAGCAGGTGGT GAAGTTCTG

NanoString

X. maculatus Jp 163 B skin samples were used in a microarray analysis at the Baylor College of Medicine Microarray Core Facility (Houston, TX). RNA isolated from *X. maculatus* skin was used as nCounter input (500 ng RNA). Hybridization protocols were strictly followed according to manufacturer's instructions (Geiss *et al*., 2008) with 7 µL of RNA solution (71.4 ng/ µL). Hybridized samples were incubated overnight at 65°C with a custom set of probes in the NanoString Prep Station and immediately evaluated with the NanoString nCounter based on color code signals. Data analysis was performed by lane normalization using a set of standard NanoString probes followed by sample normalization using a set of 10 housekeeping genes. Counts were generated by nCounter

Digital Analyzer. Fold changes were calculated on normalized counts and plotted using Microsoft Excel. Two biological samples previously used in RNA-Seq analysis were selected for NanoString.

Table 2-3: NanoString custom designed probe set for 19 test targets and 10 housekeeping controls. Asterisked genes represent housekeeping genes.

Gene Name	Ensembl ID	Target Sequence (5'-3')
klhl38b	ENSXMAT00000008690	TTTTGAGACACTTATTGGTTGGATCCGTCATGAT CCCGTCTCCAGGCGGGGGACCATAAGCAGCCTT TTCAAAAAGGTCCGTCTTCGACATTTACACCCT
clock	ENSXMAT00000017010	CCCAGCAGGGCCAGACTCAGACCATCAGCATTT CTCAGCAGCAGGAGCAGCAGCAGCAGATTCAG GTGCAGAACCAGGTTTCCGCGCTGCAGGCAGGT CA
cry2a	ENSXMAT00000009327	CCTGCAGCTGTCTCTTACATCACCTCTGAAACTC TTTACCTCCACCTCTCCCACCTACACTCACCATT CACCAGCTTTGAATGCCTCAGCAGTCTGTTTA
ppp1r27	ENSXMAT00000018069	AGGTCCCTTGAGAATCACAGTCGTCCGAAAGCC GCTGCAAGTTCTTCGGCGGTGAACGGAGAAAGC CGCATCAGTCCAGGTTCCTGGTTTTTGAGCTGCC
ccnf	ENSXMAT00000004757	AGCTCAGGATACTCATCTGTCCAGAGTGTTAGC CCATCATCTACATGCTCCTCGTCCTCCCTCGTGA CCCACACGTTCAGGACCTTTACCACATCACTTG
spc25	ENSXMAT00000011885	TTTAAAAGGAAGGCCAAAGAAATGTGGACTAA CTGTATGCTAATGATCTCAAATAGTGATGCTGG CCTTAAGAAGTAATTGATACTCTGGTCTGTAAC CG
fggy	ENSXMAT00000018361	AAAGCCGCTCACTTTTTTGACCTGCCGGACTTCC TGTCCTGGAAAGCTACAGGCTCCACAACGAGGT CTTTATGTACTCTAGTGTGTAAGTGGACATACT
raver1	ENSXMAT00000000218	CAGCACAAGGAGTATCGATGCTAGGGGATCTTC CTAAAGAGATGAACCTTCCTCAGAGCGCCTTTC TCAATGCCAATGTTTATCCTTCAGCGAGCAGCA G
kifc1	ENSXMAT00000016886	GAGTCTCATACGGGTAAAACGGCCGACACACAG AAGAATTATCACTTCAGTTTCGACCGGGTGTTC GGGCCTCTGGCTTCACAGCAGGAGATCTTTGAT G
arhgap19	ENSXMAT00000014517	GCTCCCTCCAGCCGCCAGTAAGAAGCATCCTCG TTCCCGCTCCTTTGGTGGCTTTATCAAGCGAAAA GCTCGAGGCGAGCAGATGAGAGAGAGGCACAT C

Table 2-3-Continued: NanoString custom designed probe set for 19 test targets and 10 housekeeping controls. Asterisked genes represent housekeeping genes.

Gene Name	Ensembl ID	Target Sequence (5'-3')
numa1	ENSXMAT00000011193	AATCAATCTCTCCAGTCTGCAACAGACCAAGT CTTGGCTAAAGAAAACCTGCTAGCTCAGAAG GACACTGAAATTTCCCAGCAAAACGATTCACT TCAAA
cdk1	ENSXMAT00000014787	AAGGGACCTATGGGGTGGTGTATAAGGGCAG ACATAAGTCCACAGGACAAGTTGTGGCTATGA AGAAAATCCGTCTGGAGAGCGAGGAGGAGGG AGTTCC
mad2l1	ENSXMAT00000017587	TGAGATCCGCTCTGTCATCAGGCAGATAACAG CCACGGTTACCTTCCTCCCTCTGCTGGAGACG CCGTGTGCCTTTGATCTCCTGGTCTACACTGAT AAA
bhlhe40	ENSXMAT00000002257	CAGAGTGGCATGCAAATCGAGCAACCCACTG TTAGCCAGGAGAAGTCAGAGGAGATGTTTCG CTCTGGTTTCCACATGTGTGCCAAGGAGATTC TCCAGT
parpbp	ENSXMAT00000017412	AAACAACAAAAGAGCTAAAAGAGAGGATTGT CCAGCTTCACCAGACCCAGAAACAAGCTGCTA ATGTGGATGGGACGGGTATAAGTCCTGCTAGG CCAAA
kpna2	ENSXMAT00000008371	AGGTGTTGGCCGACGCGTGCTGGGCCGTTTCC TACCTTACGGACGGACCCAACGACCGCATTGA CGTGGTGGTCAAAACCGGCGTGATTCCTCGCC TGGT
pif1	ENSXMAT00000003968	TCTTCACTGGAAGTGCTGGTACGGGGAAATCC TTCCTGCTGAAGAGAATCCTGGGATCTCTCCC ACCGAAGAGCACCTTTGCTACGGCCAGCACA GGAGT
cdca7a	ENSXMAT00000005334	CTAAGACTGTAAGCTATAACTGAGCAAAAAA TTGCCCAGTACACCATCCGCAGTCTTACCTGT GATGAAATGCAATAGTCCTGTGATGTTAGCAT TGCCT
TPM4*	ENSXMAT00000000653	ATCCTGAATGACAGACTCAAGGAGGCGGAAA CCCGTGCAGAATTTGCAGAAAGGACGGTGTC AAAGCTTGAAAAGACCATAGACGACCTAGAA GAGAACC
fam102bb*	ENSXMAT00000000552	GTGATGAAGCATTAGCGCTGCGATGACAGGA TGACCTTGATCACACTTTAAACAAATGGTTTG CGTTGGTTTCTCAATTCCCACAGCAAACACAA CGCCC

CHAPTER III

CO-INDUCED MODULATION OF GENE EXPRESSION IN *XIPHOPHORUS MACULATUS* JP 163 B SKIN

Introduction

Messenger RNA (mRNA) is synthesized in the nucleus of a cell from a complementary DNA strand, exported to the cytoplasm to the ribosomes where it is used to synthesize proteins. Advancements in genetic sequencing technology and bioinformatic tools have allowed scientists to observe each transcript synthesized from each gene in a mapped genome for a given tissue sample. The mRNA transcripts synthesized reflect the needs of a cell (e.g. interleukins synthesized to cope with an inflammatory response; Erchler and Keller, 2000). Thus, the total number of transcripts in a tissue can reflect the initial state, or a genetic response, of that tissue to an external stimulus, such as full spectrum (i.e. CO) light.

To understand global gene expression in response to varying CO doses the number of genes in skin that significantly changed in expression (i.e. modulated) after each exposure was evaluated by comparison with RNA from the skin of unexposed fish. The number of genes shared (up and down-modulated) between various exposure sets may implicate a shared response, while the number of unique genes may implicate a response that is novel to a particular exposure. This evaluation was used to assess the response shared by all doses.

Results

A. Differential Gene Expression in Response to CO Exposure

An overview of the number of genes differentially expressed (DE) in 10,000 K (CO) light exposed skin at various times, compared to skin from unexposed from sibling *X. maculatus* Jp 163 B males, based on RNA-Seq analysis (i.e. transcript presence modulated up or down) is shown in **Fig 3-1**. The total number of genes DE after 20 min. was 380 (139 up/241 down); after 40 min., 340 (104 up/240 down); after 60 min., 327 (100 up/227 down); and after 80 min., 141 (54 up/87 down). All exposures exhibit and overall differential expression patterns of more down-modulated genes than up-modulated genes.

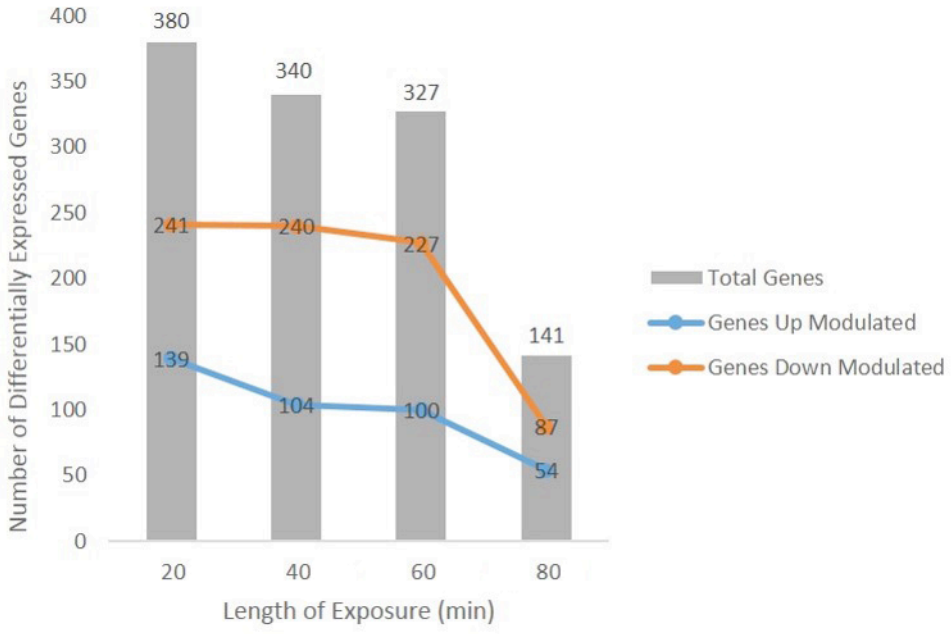

Fig. 3-1: Differentially expressed (DE) genes (±2 fold change, *p*-adj. ≤ 0.01) in the skin of male *X. maculatus* Jp 163 B in response to CO exposure. Numbers of DE genes total (grey), up-modulated (blue) and down-modulated (orange) following CO dosage are shown. Data are derived from RNA obtained from two individual animals after live fish exposure to CO light.

B. Genetic Responses Among CO Exposures

Gene sets were compared between increasing doses to assess what fraction of genes were shared as CO dosage increased. A comparison of the 20 and 40 min. gene sets revealed a both doses had a total of 217 DE genes (64%) in common (i.e. shared) (39 up/178 down, 38% up/ 74% down) between 20 and 40 min. A 40 vs. 60 min. gene set comparison revealed a total of 206 DE genes (63%) were shared (32 up/174 down, 32% up/ 77% down) between 40 and 60 min. Comparison of the 60 and 80 min. gene sets revealed a total of 94 DE genes (67%) were shared (14 up/80 down, 26% up/ 92% down) between the 60 and 80 min. exposures.

Six DE up-modulated genes and seventy-three DE down-modulated genes (79 total) were shared (21%, 23%, 24% and 56%) between all four exposures (20, 40, 60 and 80 min., respectively). Given the reduction in DE genes at 80 min. and the similarity in the number at 20, 40 and 60 min., the 20, 40 and 60 min. gene sets were evaluated for the fraction of shared genes. One hundred-eighty one DE genes (20 up-modulated and 161 down-modulated) were shared by the 20, 40 and 60 min. gene sets. All 79 genes that are shared with all four of the time points are found within the 181 genes shared among 20, 40 and 60 min. All comparisons exhibit differential expression patterns sharing more down-modulated genes than up-modulated genes.

Table 3-2 shows the unique responses among comparison of 20 and 40 min., 164 DE genes (43%) were unique to the 20 min. exposure (100 up/64 down, 72% up/ 27% down), while 89 DE genes (26%) were unique to the 40 min. exposure (63 up/26 down, 61% up/ 11% down). Among the 40 and 60 min. comparison, 138 DE genes (41%) were unique to the 40 min. exposure (72 up/66 down, 69% up/ 28% down), while 121 DE

genes (37%) were unique to the 60 min. exposure (68 up/53 down, 68% up/ 23% down). Among the 60 and 80 min. comparison, 233 DE genes (71%) were unique to the 60 min. exposure (86 up/ 147 down, 86% up/ 65% down), while 47 DE genes (33%) were unique to the 80 min. exposure (40 up/7 down, 74% up/ 8% down).

An additional comparison of each individual exposure to the 20 up-modulated and 161 down-modulated genes shared by 20, 40 and 60 min. was used to assess the unique response of each exposure (**Table 3-3**). One hundred ninety- nine DE unique genes (52%) were revealed (119 up/ 80 down, 86% up/ 33% down) after 20 min. of exposure. One hundred sixty-three DE unique genes (48%) were revealed (84 up/79 down, 81% up/ 33% down) after 40 min. of exposure. One hundred forty-six DE unique genes (45%) were revealed (80 up/66 down, 80% up/ 29% down) after 60 min. of exposure. Sixty-two DE unique genes (44%) were revealed (48 up/14 down, 89% up/ 16% down) after 80 min. of exposure.

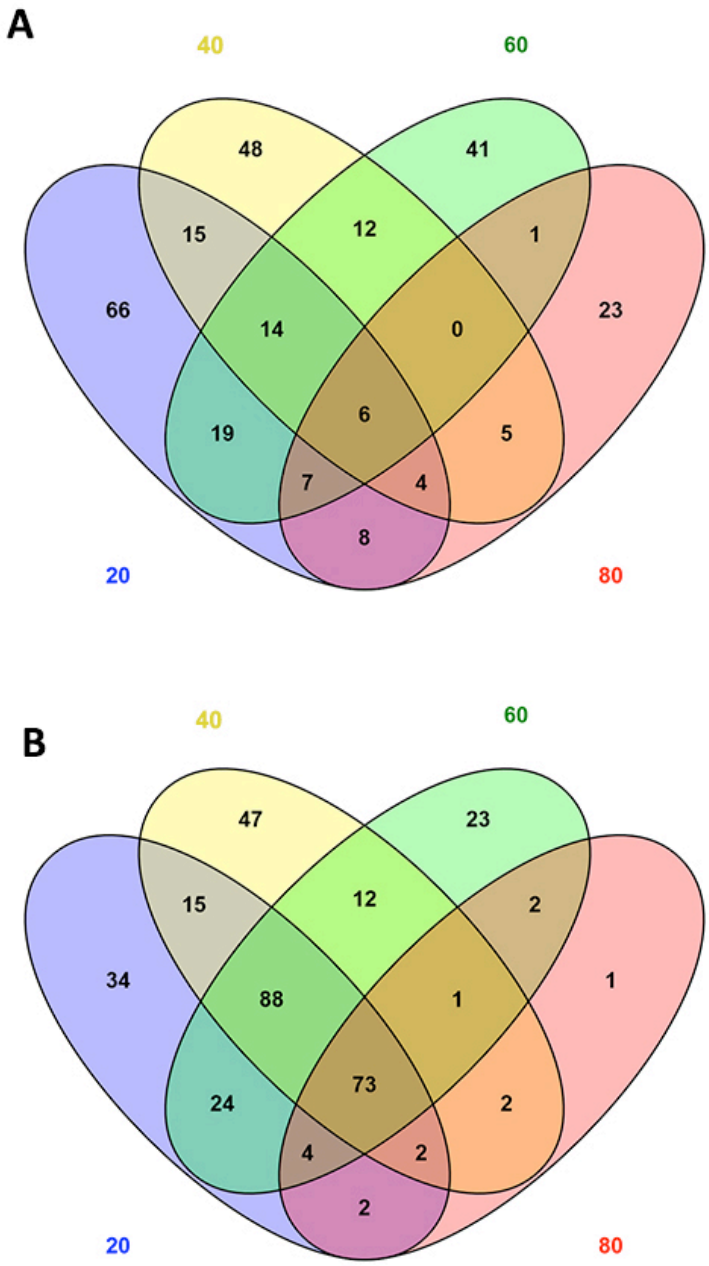

Fig. 3-2: Venn diagram representing the number of shared and unique up (panel A) and down (panel B) DE genes (±2 fold change, *p*-adj < 0.01) between CO exposures. Genes differentially expressed after 20 min. are located in the blue oval, after 40 min. in the yellow oval, after 60 min. in the green oval and after 80 min. in the red oval. Genes shared by all four exposures (6 up/ 73 down) are located in the center of each diagram (dark yellow). Genes shared by 20, 40 and 60 min. exposures are located on the left (14 and 6 up/ 88 and 73 down). Unique genes are comparison dependent.

Table 3-1: Table showing the fractions of DE up and down-modulated shared genes (p-adj < 0.01, ±2 fold change) for comparisons of the 20, 40 and 60 min. gene sets.

Comparison (min)	# Shared Genes-Up	# Shared Genes-Down	Total # Genes Shared	% Shared Genes-Up	% Shared Genes-Down	% Genes Shared
20 vs. 40	39	178	217	38%	74%	64%
40 vs. 60	32	174	206	32%	77%	63%
60 vs. 80	14	80	94	26%	92%	67%

Table 3-2: Table showing the fractions of DE up and down-modulated unique genes (p-adj < 0.01, ±2 fold change) for various comparisons of the 20, 40, 60 and 80 min. gene sets. Bolded time points indicate the exposure for which the unique gene statistics are given.

Comparison (min)	# Unique Genes-Up	# Unique Genes-Down	Total # Unique Genes	% Unique Genes-Up	% Unique Genes-Down	% Unique Genes
20 vs. 40	100	64	164	72%	27%	43%
20 vs. **40**	63	26	89	61%	11%	26%
40 vs. 60	72	66	138	69%	28%	41%
40 vs. **60**	68	53	121	68%	23%	37%
60 vs. 80	86	147	233	86%	65%	71%
60 vs. **80**	40	7	47	74%	8%	33%

Table 3-3: Table showing the fractions of unique DE up and down-modulated genes (p-adj < 0.01, ±2 fold change) for 20, 40, 60 and 80 min. when compared to the 181 overall shared gene set.

Comparison (min. vs shared # of genes)	# Unique Genes-Up	# Unique Genes-Down	Total # Unique Genes	% Unique Genes-Up	% Unique Genes-Down	% Unique Genes
20 vs. 181	119	80	199	86%	33%	52%
40 vs. 181	84	79	163	81%	33%	48%
60 vs. 181	80	66	146	80%	29%	45%
80 vs. 181	48	14	62	89%	16%	44%

Discussion

The total number of DE genes that met the statistical cut-off is similar after 20, 40, and 60 min. of exposure, but declines approximately 2.5 fold in response to 80 min. of CO, compared to any of the other three doses. The 80 min. experimental samples exhibit similar read count statistics to other samples used in this experiment (**Table 2-1**), thus observed difference in number of DE genes are not attributed to abnormalities in read data. The reduction could be attributed to adaptation of the epithelial cells to CO exposure. In general, cells respond to abrupt changes in their environment by adjusting their physiology and metabolism (López-Maury *et al*., 2008). This generally requires synthesis of additional or new proteins and thus a change in gene expression. Modulated gene expression levels, in a general eukaryotic cell, return to or nearly basal expression levels if a cell can adapt to the external stimulus (López-Maury *et al*., 2008).

Comparisons of various exposures exhibit a similar percentage of shared DE up and down-modulated genes. In these data the large number of shared DE down-modulated genes in all comparisons reflect a shared response, while the DE up-modulated genes exhibit a greater unique response for each exposure time, sharing only 38%, 32% and 26% of DE genes, respectively (**Table 3-1**). While UV-light is known to cause suppression of certain biological functions in humans (Maverakis *et al*., 2010), the impact of visible light, or full spectrum light have not been characterized as thoroughly. Exposure to visible light is known to suppress expression of some genes (Czeisler, *et al.* 1995; Myers *et al*. 1996), however large scale suppression by light has not been described in the literature. Suppression of gene expression is a regulatory feature of genetic pathways that can impact both the expression of genes downstream of those suppressed

and influence a biological function (e.g. tumor growth; Sebolt-Leopold *et al*., 1999). This possibility will be addressed in chapter 4, where we report and discusses the biological functions of the DE gene sets presented here.

Among the various comparisons of DE gene sets, all sets of DE up-modulated genes are 60% unique (i.e. not shared). Comparions of each exposure set to the overall 181 shared gene set exhibit a more unique response in the up-modulated genes, all exhibiting an 80%, or greater, percentage of unique DE up-modulated genes. These data combined suggest each exposure point has a response that is novel from both the overall shared response and from the other exposures.

CHAPTER IV

CHARACTERIZATION OF BIOLOGICAL FUNCTIONS MODULATED BY FULL SPECTRUM FLUORESCENT LIGHT EXPOSURE IN *XIPHOPHORUS MACULATUS* JP 163 B SKIN

Introduction

We have presented shared and unique DE gene fractions in the skin of *X. maculatus* for several timed exposures to full spectrum fluorescent light (CO; see Chapter 3). Within the gene set of each individual exposure and within the gene set of the overall shared response over half of the significant DE genes exhibited down-modulation of expression. Down-modulation of nearly 200 genes could possibly result from suppression of a single genetic pathway but, given that genes can be involved in more than one functional process, it is more likely the fraction of down-modulated genes represents suppression of several pathways or cellular functions. Additionally, each dose appeared to generate a novel response when compared to either other exposures or to the overall shared response. This indicates up-modulation of some pathways or functions is dependent on the exposure dose. Examples of this dose specific pathway induction have been previously characterized in *Xiphophorus* with increasing doses of UV-B light (Yang *et al.,* 2014).

To better understand what functions are modulated by CO, both overall and in response to each exposure time, we used bioinformatic software available in the public domain (i.e., DAVID Gene Ontology; http://david.abcc.ncifcrf.gov/ and GeneMania; www.genemania.org). In these analyses we analyzed 181 genes (20 up-modulated/ 161 down-modulated) shared between 20, 40 and 60 min. to assess the overall shared

response to CO. Following analysis of the overall shared response, the 181 shared gene set was eliminated from the 20, 40 and 60 min. sets to asses any novel response elicited by these individual doses. Previously, we had shown 79 DE genes were shared between all four exposures (**Fig. 3-2**; including the 80 min exposure). These 79 DE genes are a subset of the 181 shared gene set derived from the 20, 40, and 60 min. exposures (**Table 4-a** & **Table 4-b**). These genes were considered to be part of the overall shared response and thus not discussed separately.

Results

A. Functional Clusters of the Shared Genetic Response

1) Up-regulated Genes in the Shared Gene Set.

As previously stated, 181 significant DE genes were shared overall between the 20, 40 and 60 min. gene sets. Twenty of these genes were up-modulated, thus composed the overall up-modulated response. DAVID bioinformatic analysis of the overall up-modulated gene set resulted in the generation of 2 functional clusters. Six genes were clustered by "rhythmic process", while two genes were clustered by "cytoskeletal anchoring at plasma membrane" (**Table 4-2**). Network visualization of these 8 genes revealed physical interactions and shared protein domains with queried and predicted genes, but not genetic interactions[1].

2) Down-regulated Genes in the Shared Gene Set.

DAVID bioinformatic analysis of the overall down-modulated gene set (161 genes) resulted in the generation of 13 functional clusters with enriched p-values < 0.01.

[1] Genemania describes a genetic interaction as a modification in expression for one gene that is caused by modification in expression for another gene (Warde-Farley *et al*., 2010).

One hundred twenty-one unique genes were clustered among “cell cycle”, “DNA metabolic processes”, “microtubule-based process”, “chromosome segregation”, “response to DNA damage stimulus”, “phosphoinositide-mediated signaling”, “DNA packaging”, “cell proliferation”, “protein-DNA complex assembly”, “negative regulation of cell component organization”, “L-serine metabolic process”, “cellular macromolecular complex subunit organization”, and “protein amino acid phosphorylation” (**Table 4-3**). Sixty-nine genes from the cell cycle cluster, the largest cluster, also appeared in at least one of the other 12 functional clusters. Thus, this list was used for closer evaluation of shared domains. Six clusters of genes related by shared protein domain were identified via a gene network (cyclins, helicases, kinases, kinesins, minichromosome maintenance and transcription factors) (**Fig. 4-3**).

Table 4-1: Eight of the nineteen overall up-modulated genes clustered into 2 separate GO clusters.

GO ID	Description	*p*-Value	# Genes	Genes
GO:0048511	rhythmic process	1.95E-07	6	ARNTL, ARNTL2, CLOCK, CRY2, NFIL3, NPAS2
GO:0007016	cytoskeletal anchoring at plasma membrane	8.84E-03	2	SPTBN4, TLN2

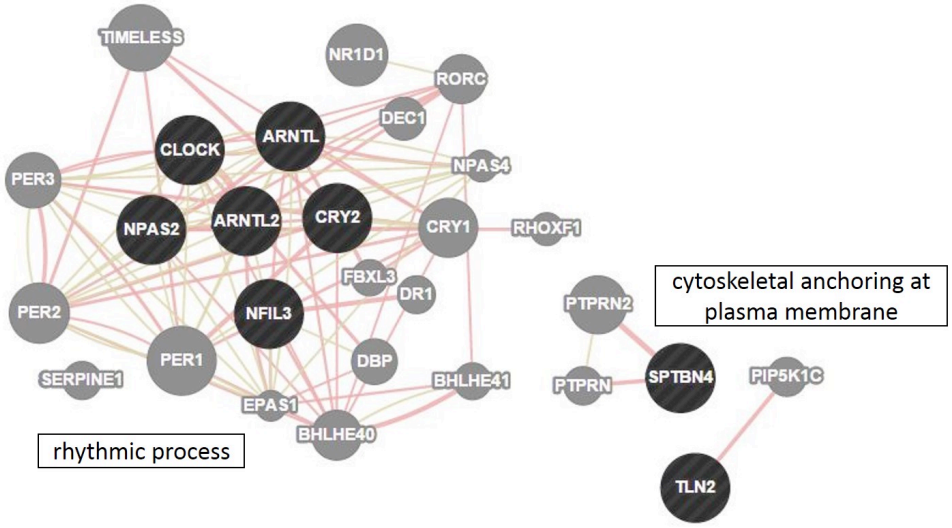

Fig. 4-1: Gene network (www.genemania.org) derived from 8 of the 19 DE up-modulated genes identified from DAVID (http://david.abcc.ncifcrf.gov/) that are shared overall between 20, 40 and 60 min. CO exposures. Queried genes are presented as black nodes. Predicted Genemania genes are presented as grey nodes. Yellow lines indicate gene products share a protein domain. Red lines indicate a physical interaction between gene products. DAVID derived GO clusters are differentiated by labels.

Table 4-2: One hundred twenty-one of one hundred-sixty one overall down-modulated genes clustered into 13 GO categories that met the cut off for functional clusters (p-value < 0.01, list not repeated). Proteins that share a protein domain in the cell cycle category are colored by family. Purple indicates kinases, green indicates cyclins, blue indicates transcription factors, red indicates helicases, pink indicates kinesin families, while orange indicates minichromosome maintenance (MCM) complex.

GO ID	Description	p-Value	# Genes	Genes
GO:0007049	cell cycle	1.28E-57	72	ANLN, **AURKA, AURKB**, **BUB1**, **BUB1B**, **CCNA2, CCNB1, CCNB3**, CDC20, CDC6, **CDC7**, CDCA8, **CDK1**, **CDK2**, CENPF, CENPJ, CHAF1A, **CHEK1**, CHTF8, CLSPN, DLGAP5, DSCC1, DSN1, **E2F7**, **E2F8**, **ERCC6L**, ESCO2, ESPL1, GTSE1, HAUS1, HAUS2, HAUS5, HAUS8, **HELLS**, INCENP, **KIF15**, **KIF18A**, **KIF22**, **KIF23**, **KIF2C**, **KIFC1**, KPNA2, MAD2L1, **MCM2**, **MCM6**, MIS12, MKI67, MTBP, NCAPH, NDC80, NUMA1, NUSAP1, **PBK**, PHGDH, **PKMYT1**, **PLK1**, POLE, PRC1, PTTG1, RACGAP1, RAD52, RBBP8, **RPA1**, SASS6, SGOL1, SMC2, SPC24, TACC3, TPX2, **TTK**, UBE2C, ZWILCH

Table 4-2-Continued: One hundred twenty-one of one hundred-sixty one overall down-modulated genes clustered into 13 GO categories that met the cut off for functional clusters (p-value < 0.01, list not repeated). Proteins that share a protein domain in the cell cycle category are colored by family. Purple indicates kinases, green indicates cyclins, blue indicates transcription factors, red indicates helicases, pink indicates kinesin families, while orange indicates minichromosome maintenance (MCM) complex.

GO ID	Description	p-Value	# Genes	Genes
GO:0006259	DNA metabolic process	5.87E-29	42	CDC6, CDC7, CDK2, CENPF, CHAF1A, CHEK1, CHTF8, CLSPN, DSCC1, DTL, EME1, ESCO2, FEN1, GINS2, GINS3, GINS4, HELLS, HMGB1, HMGB2, KIF22, KPNA2, MCM10, MCM2, MCM5, MCM6, NUDT1, PCNA, POLA2, POLD2, POLE, POLE2, PRIM2, PTTG1, RAD52, RBBP8, RNASEH2A, RPA1, RPA2, RRM1, RRM2, TOP2A, TYMS
GO:0007017	microtubule-based process	1.89E-18	25	AURKA, BUB1B, CENPJ, ESPL1, GTSE1, HAUS1, HAUS2, HAUS5, HAUS8, KIF15, KIF18A, KIF20A, KIF22, KIF23, KIF2C, KIF4A, KIFC1, KPNA2, NDC80, NUSAP1, PRC1, SASS6, TACC3, TTK, UBE2C
GO:0007059	chromosome segregation	9.21E-18	17	CENPF, DLGAP5, DSCC1, DSN1, ESPL1, INCENP, KIF18A, KIFC1, MAD2L1, MIS12, NCAPH, NDC80, NUSAP1, PTTG1, SGOL1, SMC2, TOP2A
GO:0006974	response to DNA damage stimulus	1.42E-14	25	CCNA2, CDK1, CHAF1A, CHEK1, CLSPN, DTL, EME1, ESCO2, FEN1, GTSE1, HMGB1, HMGB2, KIF22, NUDT1, PCNA, POLD2, POLE, POLE2, PTTG1, RAD52, RBBP8, RPA1, RPA2, TOP2A, TYMS
GO:0048015	phosphoinositide-mediated signaling	1.01E-06	9	AURKA, BUB1B, FEN1, HMGB2, NDC80, PCNA, TOP2A, TYMS, UBE2C
GO:0006323	DNA packaging	7.62E-05	8	CHAF1A, HELLS, HMGB2, MCM2, NCAPH, NUSAP1, SMC2, TOP2A
GO:0008283	cell proliferation	1.19E-04	14	BUB1, BUB1B, CENPF, DLGAP5, E2F8, HELLS, KIF15, KIF2C, MKI67, PCNA, PLK1, RACGAP1, TACC3, TPX2
GO:0065004	protein-DNA complex assembly	1.23E-03	6	CENPF, CHAF1A, HELLS, HMGB2, MCM2, MIS12
GO:0051129	negative regulation of cellular component organization	1.58E-03	7	BUB1, CENPF, ESPL1, HMGB1, MAD2L1, MID1IP1, TTK
GO:0006563	L-serine metabolic process	2.08E-03	3	PHGDH, PSAT1, SHMT1

Table 4-2-Continued: One hundred twenty-one of one hundred-sixty one overall down-modulated genes clustered into 13 GO categories that met the cut off for functional clusters (*p*-value < 0.01, list not repeated). Proteins that share a protein domain in the cell cycle category are colored by family. Purple indicates kinases, green indicates cyclins, blue indicates transcription factors, red indicates helicases, pink indicates kinesin families, while orange indicates minichromosome maintenance (MCM) complex.

GO ID	Description	*p*-Value	# Genes	Genes
GO:0034621	cellular macromolecular complex subunit organization	4.25E-03	10	ANLN, CENPF, CENPJ, CHAF1A, HELLS, HMGB2, KIF18A, KIF2C, MCM2, MIS12
GO:0006468	protein amino acid phosphorylation	5.77E-03	14	AURKA, AURKB, BUB1, CDC7, CDK1, CDK2, CHEK1, MELK, PASK, PBK, PKMYT1, PLK1, PLK4, TTK

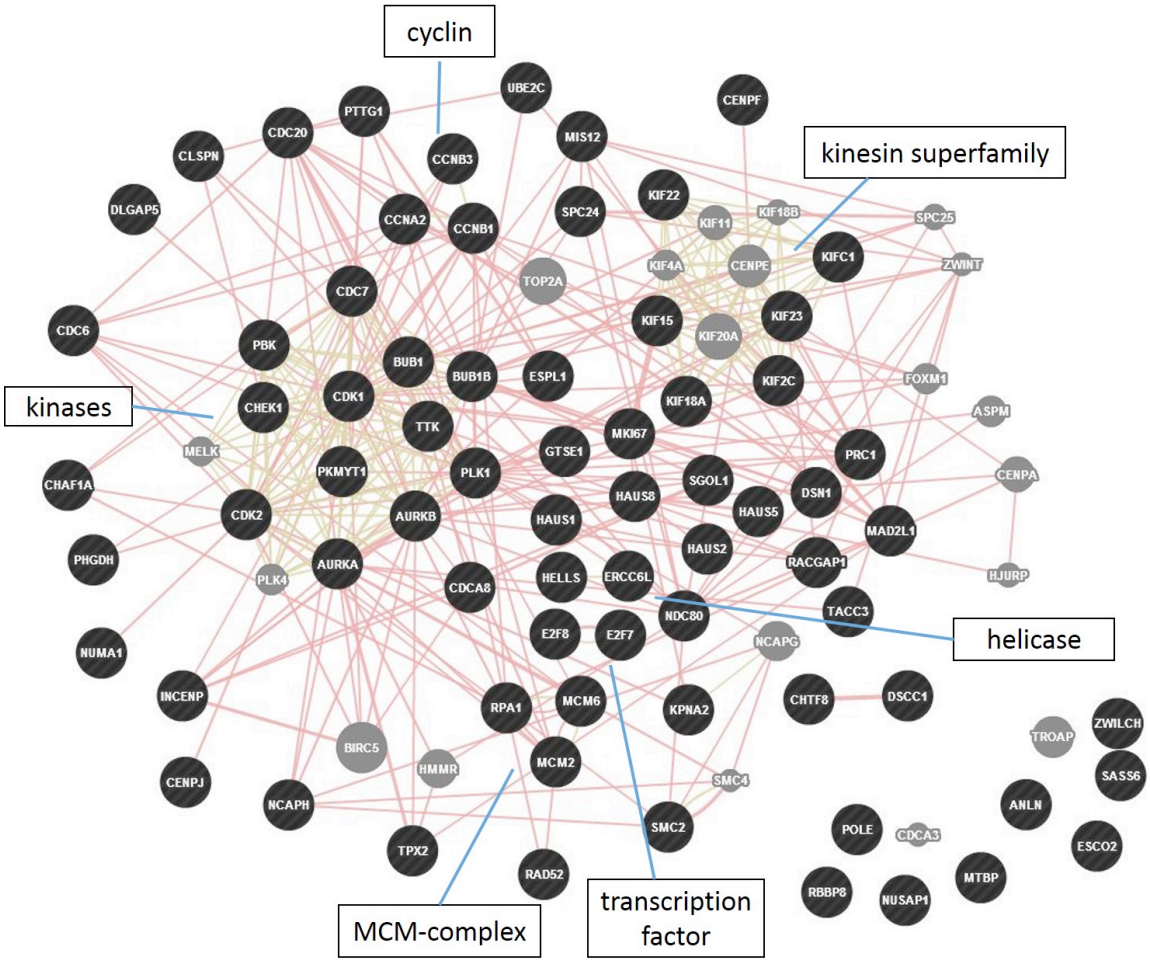

Fig. 4-2: Gene network derived from GeneMania (www.genemania.org) representing 72 DE shared down-modulated cell cycle genes derived from DAVID bioinformatic analysis of the shared between 20, 40 and 60 min. of exposure. Queried genes are presented as black nodes. Predicted genes are presented as grey nodes. Yellow lines indicate gene products share a protein domain. Red lines indicate a physical interaction between gene products. DAVID derived shared domain clusters are differentiated by labels.

Table 4-a: Table exhibiting gene name, Ensembl transcript ID, fold change, *p*-adj, and read counts of 6 significant DE 80 min. up-modulated genes that were found in common with the overall shared response. Where genes have been duplicated in *Xiphophorus*, information for both copies are presented.

Gene ID	Ensembl id	*p*-adj.	Fold Change	Avg. Read Counts
ucp2	ENSXMAT00000011982	7.3E-09	4.2	667.3
npas2	ENSXMAT00000012307	9.4E-03	3.3	157.4
cdkn1d	ENSXMAT00000004312	1.3E-05	3.1	3466.4
pfkfb2b	ENSXMAT00000017816	3.0E-03	2.6	308.1
arntl2 (1 of 2)	ENSXMAT00000001499	2.5E-04	2.6	1998.8
nfil3-2	ENSXMAT00000019605	9.5E-03	2.5	226.1

Table 4-b: Table exhibiting gene name, Ensembl transcript ID, fold change, *p*-adj, and read counts of 73 significant DE 80 min. down-modulated genes that were found in common with the overall shared response. Where genes have been duplicated in *Xiphophorus*, information for both copies are presented.

Gene ID	Ensembl id	*p*-adj.	Fold Change	Avg. Read Counts
ccna2	ENSXMAT00000002065	8.1E-03	-2.3	901.7
abhd2a	ENSXMAT00000002347	1.0E-02	-2.3	2992.9
hmgb1a	ENSXMAT00000008441	7.5E-03	-2.3	14085.0
rrm2	ENSXMAT00000009953	5.3E-03	-2.3	4165.4
rrm1 (2 of 2)	ENSXMAT00000010434	8.6E-03	-2.3	790.4
ercc6l	ENSXMAT00000000938	6.1E-03	-2.5	365.1
espl1	ENSXMAT00000002159	5.3E-03	-2.5	656.2
tyms	ENSXMAT00000002247	6.8E-03	-2.5	530.8
tdh	ENSXMAT00000004246	4.1E-03	-2.5	1121.7
fen1	ENSXMAT00000006142	3.5E-03	-2.5	529.3
tacc3	ENSXMAT00000013574	3.1E-03	-2.5	800.0
mad2l1	ENSXMAT00000017587	6.6E-03	-2.5	408.1
shcbp1	ENSXMAT00000001162	6.1E-03	-2.6	287.0
gins2	ENSXMAT00000003130	4.0E-03	-2.6	369.0
kif23	ENSXMAT00000003706	2.3E-03	-2.6	580.3
smc2	ENSXMAT00000004597	1.2E-03	-2.6	1775.2
chtf8	ENSXMAT00000006190	6.1E-03	-2.6	268.4
pbk	ENSXMAT00000006368	3.1E-03	-2.6	283.8
kiaa0101	ENSXMAT00000006710	3.5E-03	-2.6	362.5
ttk	ENSXMAT00000007097	9.3E-04	-2.6	884.3

Table 4-b-Continued: Table exhibiting gene name, Ensembl transcript ID, fold change, *p*-adj, and read counts of 73 significant DE 80 min. down-modulated genes that were found in common with the overall shared response. Where genes have been duplicated in *Xiphophorus*, information for both copies are presented.

Gene ID	Ensembl id	*p*-adj.	Fold Change	Avg. Read Counts
acrc	ENSXMAT00000009551	3.6E-03	-2.6	396.5
fam64a	ENSXMAT00000010766	3.1E-03	-2.6	543.7
top2a	ENSXMAT00000011402	4.9E-04	-2.6	1821.7
chaf1a	ENSXMAT00000011902	2.6E-03	-2.6	498.5
ticrr	ENSXMAT00000013162	5.3E-03	-2.6	230.7
mki67	ENSXMAT00000014672	6.4E-04	-2.6	3460.0
kif2c	ENSXMAT00000015773	2.2E-03	-2.6	659.0
cdk1	ENSXMAT00000014787	1.2E-04	-2.8	2062.7
cenpk	ENSXMAT00000000137	2.3E-03	-2.8	258.4
incenp	ENSXMAT00000003900	2.7E-04	-2.8	1542.7
tpx2	ENSXMAT00000004496	2.1E-04	-2.8	1283.8
kif4a	ENSXMAT00000005069	4.0E-04	-2.8	1019.5
bub1bb	ENSXMAT00000006585	6.7E-04	-2.8	334.8
ncaph	ENSXMAT00000010239	5.1E-04	-2.8	720.9
racgap1 (1 of 2)	ENSXMAT00000012026	5.1E-04	-2.8	705.7
plk4	ENSXMAT00000013616	1.7E-03	-2.8	429.5
dlgap5	ENSXMAT00000014915	4.3E-04	-2.8	1008.7
net1 (2 of 2)	ENSXMAT00000016979	1.7E-03	-2.8	399.9
kif22	ENSXMAT00000018645	2.1E-04	-2.8	666.5
cdca7b	ENSXMAT00000000581	5.9E-03	-3.0	129.6
numa1	ENSXMAT00000011193	2.1E-04	-3.0	496.1
adm2a	ENSXMAT00000005147	3.4E-03	-3.0	154.9
anln	ENSXMAT00000007460	2.6E-05	-3.0	2635.9
knstrn	ENSXMAT00000007687	1.7E-03	-3.0	235.9
hmmr	ENSXMAT00000010557	5.1E-04	-3.0	315.2
ube2c	ENSXMAT00000012443	2.6E-04	-3.0	903.7
plk1	ENSXMAT00000012882	6.0E-05	-3.0	1301.3
kif20a	ENSXMAT00000012995	1.9E-04	-3.0	784.5
arhgap19	ENSXMAT00000014517	4.3E-03	-3.0	130.7
cenpf	ENSXMAT00000015178	7.1E-05	-3.0	968.0
prc1b	ENSXMAT00000018132	4.5E-04	-3.0	329.1
per1b	ENSXMAT00000015376	7.7E-06	-3.2	2994.7

Table 4-b-Continued: Table exhibiting gene name, Ensembl transcript ID, fold change, *p*-adj, and read counts of 73 significant DE 80 min. down-modulated genes that were found in common with the overall shared response. Where genes have been duplicated in *Xiphophorus*, information for both copies are presented.

Gene ID	Ensembl id	*p*-adj.	Fold Change	Avg. Read Counts
dck	ENSXMAT00000005437	1.5E-04	-3.2	308.2
aurka	ENSXMAT00000006097	2.1E-04	-3.2	518.0
prc1a	ENSXMAT00000006913	3.4E-05	-3.2	726.1
melk	ENSXMAT00000012713	7.6E-05	-3.2	440.4
ccnb3	ENSXMAT00000015109	7.2E-05	-3.2	531.3
depdc1a	ENSXMAT00000000722	6.3E-04	-3.5	139.1
dscc1	ENSXMAT00000010893	1.0E-03	-3.5	125.7
parpbp	ENSXMAT00000017412	3.7E-04	-3.5	183.1
raver1	ENSXMAT00000000218	7.1E-05	-3.7	186.9
per3	ENSXMAT00000004015	1.7E-07	-3.7	5003.1
seph	ENSXMAT00000007664	2.8E-05	-3.7	313.6
kpna2	ENSXMAT00000008371	8.4E-08	-3.7	2832.3
ccnb1	ENSXMAT00000008618	3.0E-07	-3.7	1330.7
si:ch211-69g19.2	ENSXMAT00000011167	3.0E-06	-3.7	592.6
dtl	ENSXMAT00000017561	5.1E-04	-3.7	168.5
cdc20	ENSXMAT00000016054	4.0E-07	-4.0	628.6
cdc6	ENSXMAT00000014215	1.5E-05	-4.3	186.6
uncharacterized	ENSXMAT00000005927	1.8E-09	-4.6	3401.1
cdca7a	ENSXMAT00000005334	1.8E-09	-4.6	1234.9
phgdh	ENSXMAT00000014406	2.1E-09	-5.3	460.1
psat1	ENSXMAT00000002807	4.3E-10	-6.5	273.7

B. Functional Clusters After 20 min. Exposure

One hundred nineteen DE up-modulated 20 min. genes were unique from the overall DE up-modulated response. DAVID bioinformatic analysis of this gene set resulted in the clustering of 20 unique genes into 3 gene ontologies: “phosphorylation”, “transmembrane receptor protein tyrosine kinase signaling pathway” and “rhythmic process” (**Table 4-5**). Eighty DE down-modulated 20 min. genes were unique from the overall DE down-modulated response. Bioinformatic analysis of this gene set resulted in

the clustering of 32 unique genes into 4 gene ontologies: “cell cycle”, “DNA metabolic processes”, “response to DNA damage stimulus” and “chromosome organization” (**Table 4-7**).

Table 4-3: Twenty of the one hundred-nineteen up-modulated genes novel to the 20 min. exposure clustered into 3 unique GO clusters (*p*-value < 0.01, list not repeated).

GO ID	Description	*p*-Value	# Genes	Genes
GO:0016310	phosphorylation	6.89E-05	15	ABL2, ACVR1C, ATP6AP1, BCKDK, CAMKK1, EEF2K, EGFR, GHR, IGF1R, IPMK, KALRN, MKNK2, PIM1, TTBK2, UHMK1
GO:0007169	transmembrane receptor protein tyrosine kinase signaling pathway	6.78E-03	6	ATP6AP1, EGFR, EREG, GHR, IGF1R, TXNIP
GO:0048511	rhythmic process	4.79E-03	5	EGFR, EREG, HLF, NFIL3, PRF1

Table 4-4: Table showing gene name, Ensembl transcript ID, fold change, *p*-adj, and read counts of the DAVID clustered up-modulated genes novel to the 20 min. exposure. Where genes have been duplicated in *Xiphophorus*, information for both copies are presented.

Gene Name	Ensembl ID	*p*-adj.	Fold Change	Avg. Read Count
camkk1	ENSXMAT00000012015	8.6E-03	5.1	31.1
bckdk	ENSXMAT00000008840	1.0E-03	4.1	11985.3
hlfa	ENSXMAT00000016999	3.2E-03	3.7	691.0
nfil3-5	ENSXMAT00000005145	5.0E-03	3.7	6321.3
mknk2a	ENSXMAT00000002683	2.4E-07	3.4	1178.7
igf1ra	ENSXMAT00000003758	8.1E-05	3.3	371.2
ipmkb	ENSXMAT00000014591	5.3E-03	3.3	1196.2
eef2k	ENSXMAT00000015830	1.4E-04	3.0	7246.0
PRF1	ENSXMAT00000017941	1.6E-03	2.9	335.7
ttbk2	ENSXMAT00000014455	4.4E-03	2.9	12402.0
acvr1c	ENSXMAT00000011347	5.5E-03	2.7	220.6
uhmk1	ENSXMAT00000016113	5.2E-03	2.7	709.7
abl2	ENSXMAT00000003220	1.1E-03	2.5	3349.9
ghrb	ENSXMAT00000016579	1.4E-04	2.4	231.8

Table 4-4-Continued: Table showing gene name, Ensembl transcript ID, fold change, *p*-adj, and read counts of the DAVID clustered up-modulated genes novel to the 20 min. exposure. Where genes have been duplicated in *Xiphophorus*, information for both copies are presented.

Gene Name	Ensembl ID	*p*-adj.	Fold Change	Avg. Read Count
kalrnb	ENSXMAT00000000949	1.3E-05	2.4	9374.7
pim1	ENSXMAT00000016450	1.8E-03	2.3	194.6
txnipa	ENSXMAT00000003279	9.4E-03	2.3	221.8
x-egfrb	ENSXMAT00000008852	6.2E-03	2.2	734.8
ereg	ENSXMAT00000010312	5.5E-03	2.2	875.1
atp6ap1a	ENSXMAT00000000286	6.1E-03	2.1	5264.7

Table 4-5: Thirty-two of the eighty down-modulated genes novel to 20 min. clustered into 4 unique GO clusters (*p*-value < 0.01, list not repeated).

GO ID	Description	*p*-Value	# Genes	Genes
GO:0007049	cell cycle	1.29E-11	21	ASPM, CCNF, CDT1, CEP135, DBF4, DTYMK, E2F2, E2F3, GSG2, LIG1, MAP2K6, MCM3, MDC1, MSH6, PIN1, POLD1, RAD51, RAD54L, SKP2, SUV39H1, TIMELESS
GO:0006259	DNA metabolic process	1.21E-10	17	ALKBH2, C10ORF2, CDT1, CRY1, DBF4, DNMT1, LIG1, MCM3, MDC1, MSH6, NEIL3, POLD1, POLD3, RAD51, RAD54L, RECQL4, UNG
GO:0006974	response to DNA damage stimulus	2.79E-09	14	ALKBH2, CRY1, LIG1, MAP2K6, MDC1, MSH6, NEIL3, POLD1, POLD3, RAD51, RAD54L, RECQL4, TIMELESS, UNG
GO:0051276	chromosome organization	3.70E-03	8	BRD8, DNMT1, GSG2, HP1BP3, RAD54L, SMYD1, SUV39H1, MSH6

Table 4-6: Table exhibiting gene name, Ensembl transcript ID, fold change, *p*-adj, and read counts of the DAVID clustered 20 min. down-modulated genes. Where genes have been duplicated in *Xiphophorus*, information for both copies are presented.

Gene Name	Ensembl ID	*p*-adj.	Fold Change	Avg. Read Count
cry1b	ENSXMAT00000001763	6.8E-03	-2.3	1204.3
dtymk	ENSXMAT00000003774	8.7E-03	-2.3	561.7

Table 4-6-Continued: Table exhibiting gene name, Ensembl transcript ID, fold change, *p*-adj, and read counts of the DAVID clustered 20 min. down-modulated genes. Where genes have been duplicated in *Xiphophorus*, information for both copies are presented.

Gene Name	Ensembl ID	*p*-adj.	Fold Change	Avg. Read Count
pin1	ENSXMAT00000015604	4.4E-03	-2.3	1327.0
pold3	ENSXMAT00000006072	8.7E-03	-2.3	663.3
aspm	ENSXMAT00000000723	4.3E-03	-2.5	852.0
brd8 (1 of 2)	ENSXMAT00000011210	2.7E-03	-2.5	379.1
cep135	ENSXMAT00000016953	8.3E-03	-2.5	225.0
dnmt1	ENSXMAT00000018188	1.7E-03	-2.5	1931.2
map2k6	ENSXMAT00000012723	2.0E-03	-2.5	1221.6
MDC1	ENSXMAT00000011013	5.2E-03	-2.5	706.5
hp1bp3	ENSXMAT00000017782	8.2E-04	-2.6	1001.0
lig1	ENSXMAT00000005885	9.7E-03	-2.6	725.3
msh6	ENSXMAT00000011028	6.8E-04	-2.6	1268.1
pold1	ENSXMAT00000011809	1.7E-03	-2.6	685.5
timeless	ENSXMAT00000003313	1.6E-03	-2.6	433.0
ccnf	ENSXMAT00000004757	6.3E-03	-2.8	389.2
neil3	ENSXMAT00000002242	9.9E-03	-2.8	98.0
rad51	ENSXMAT00000000594	1.3E-03	-2.8	267.9
rad54l (2 of 2)	ENSXMAT00000006102	7.3E-03	-2.8	126.8
unga	ENSXMAT00000018321	7.2E-03	-2.8	189.8
C10orf2	ENSXMAT00000017712	6.9E-04	-3.0	217.8
dbf4	ENSXMAT00000006893	1.3E-03	-3.0	214.8
e2f3	ENSXMAT00000009710	2.4E-03	-3.0	155.7
rad54l (1 of 2)	ENSXMAT00000000633	1.7E-03	-3.0	162.7
skp2	ENSXMAT00000013779	7.7E-03	-3.0	92.0
cdt1	ENSXMAT00000015029	1.2E-03	-3.2	161.0
smyd1b	ENSXMAT00000016123	1.1E-04	-3.5	179.1
gsg2	ENSXMAT00000009873	9.3E-03	-3.7	53.1
mcm3	ENSXMAT00000007822	3.9E-03	-3.7	1657.9
suv39h1a	ENSXMAT00000012911	3.8E-03	-3.7	330.8
e2f2	ENSXMAT00000012609	1.4E-04	-4.0	128.5
alkbh2	ENSXMAT00000018313	4.6E-04	-9.2	35.5

C) Functional Clusters After 40 min. Exposure

One hundred-four DE up-modulated 40 min. genes were unique from the overall up-modulated response. DAVID bioinformatic analysis resulted in the clustering of 14 unique genes into 2 gene ontologies: "phosphate metabolic process and "muscle organ development" (**Table 4-9**).

Seventy-nine DE down-modulated 40 min. genes were unique from the overall down-modulated response. DAVID bioinformatic analysis resulted in the clustering of 47 unique genes into 6 gene ontologies: "cell cycle", "chromosome segregation", "DNA packaging", "DNA metabolic process", "microtubule-based process", "macromolecular complex assembly" (**Table 4-11**).

Table 4-7: Fourteen of the 104 up-modulated genes novel to the 40 min. exposure clustered into 2 unique GO clusters (p-value < 0.01, list not repeated).

GO ID	Description	p-Value	# Genes	Genes
GO:0006796	phosphate metabolic process	2.59E-03	11	ATP6AP1, BRAF, EEF2K, FGF23, IGF1R, MTMR3, PTPRN, TGFBR3, THBS1, TTBK2, TTN
GO:0007517	muscle organ development	7.56E-03	5	CPT1B, MEF2D, SVIL, TGFBR3, TTN

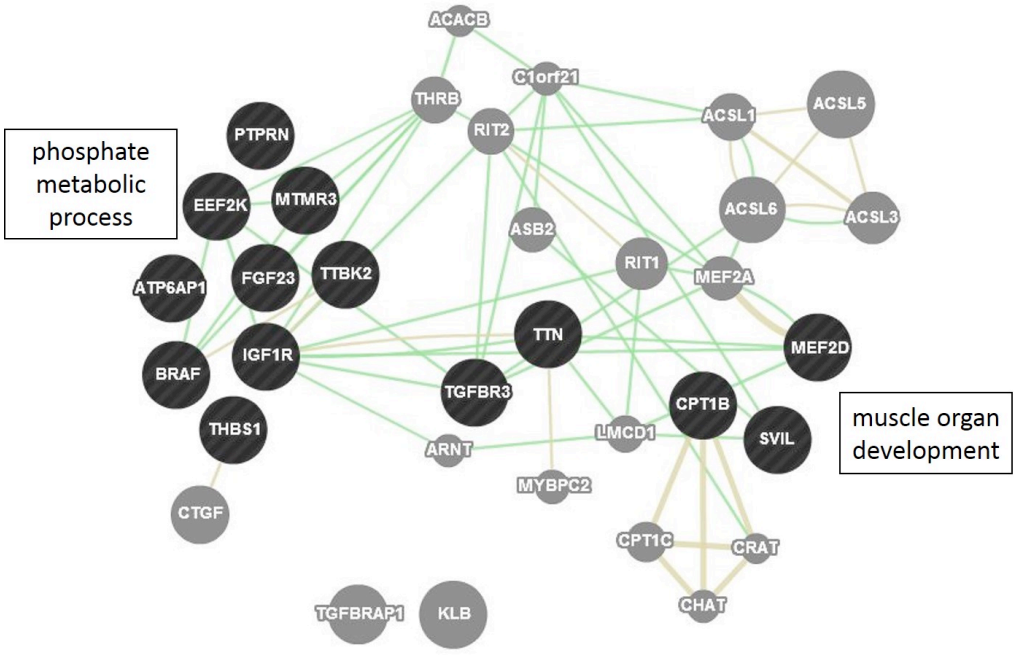

Fig. 4-3: GeneMania network representing 14 DAVID derived up-modulated genes novel to the 40 min. exposure. Queried genes are presented as black nodes. Predicted genes are presented as grey nodes. Yellow lines indicate gene products share a protein domain. Green lines indicate a modulation in expression of one gene affects another (i.e. genetic interaction). DAVID derived GO clusters are differentiated by labels.

Table 4-8: Table exhibiting gene name, Ensembl transcript ID, fold change, *p*-adj, and read counts of the DAVID clustered 40 min. up-modulated genes. Where genes have been duplicated in *Xiphophorus*, information for both copies are presented.

Gene Name	Ensembl ID	*p*-adj.	Fold Change	Avg. Read Count
fgf23	ENSXMAT00000004303	7.0E-03	12.7	16.1
ttn	ENSXMAT00000007472	4.5E-06	5.0	1470.5
cpt1b	ENSXMAT00000004684	2.3E-06	4.0	359.5
ttbk2	ENSXMAT00000014455	1.6E-04	3.3	389.8
braf	ENSXMAT00000008604	4.8E-03	3.2	126.3
tgfbr3	ENSXMAT00000011580	5.4E-04	3.0	630.0
svilb	ENSXMAT00000006021	5.4E-04	2.9	457.8
mef2d (2 of 2)	ENSXMAT00000015127	3.9E-03	2.8	343.2
igf1ra	ENSXMAT00000003758	7.0E-03	2.7	617.9
thbs1b	ENSXMAT00000007817	1.8E-03	2.7	1279.9

Table 4-8-Continued: Table exhibiting gene name, Ensembl transcript ID, fold change, *p*-adj, and read counts of the DAVID clustered 40 min. up-modulated genes. Where genes have been duplicated in *Xiphophorus*, information for both copies are presented.

Gene Name	Ensembl ID	*p*-adj.	Fold Change	Avg. Read Count
ptprna	ENSXMAT00000015992	9.6E-03	2.6	288.5
mtmr3	ENSXMAT00000004133	4.0E-03	2.5	860.0
eef2k	ENSXMAT00000015830	7.7E-03	2.4	6457.9
atp6ap1a	ENSXMAT00000000286	2.6E-03	2.2	5746.5

Table 4-9: Forty-seven of seventy-nine down-modulated genes novel to the 40 min. exposure clustered into 3 unique GO clusters (*p*-value < 0.01, list not repeated).

GO ID	Description	*p*-Value	# Genes	Genes
GO:0007049	cell cycle	4.25E-30	38	ASPM, CCNB2, CCNF, CDC45, CENPE, CEP55, CHAF1B, CIT, DDX11, E2F2, E2F3, EXO1, FAM83D, FANCD2, FANCI, FBXO5, FOXM1, GSG2, HAUS3, HAUS7, KIF20B, KNTC1, NCAPD2, NCAPD3, NCAPG, NCAPG2, NDE1, NUF2, POLD1, PSMA5, RACGAP1, RAD51, RAD54B, RAD54L, SKA1, SMC4, SPAG5, SPC25
GO:0007059	chromosome segregation	1.14E-10	10	CENPE, CENPO, DDX11, NCAPD2, NCAPD3, NCAPG, NUF2, SKA1, SMC4, SPC25
GO:0006323	DNA packaging	6.41E-08	9	CHAF1B, H2AFV, H2AFZ, HP1BP3, NCAPD2, NCAPD3, NCAPG, NCAPG2, SMC4
GO:0006259	DNA metabolic process	4.54E-07	14	BRIP1, CDC45, CHAF1B, EXO1, FANCD2, FANCI, HAUS7, POLD1, POLQ, RAD51, RAD54B, RAD54L, TK1, UNG
GO:0007017	microtubule-based process	2.13E-05	9	CENPE, FBXO5, HAUS3, HAUS7, KIF20B, NDE1, SPAG5, SPC25, TUBA1B
GO:0065003	macromolecular complex assembly	9.28E-04	11	CENPE, CHAF1B, E2F2, E2F3, FBXO5, H2AFV, H2AFZ, HP1BP3, KNTC1, RAD51, TUBA1B

Table 4-10: Table exhibiting gene name, Ensembl transcript ID, fold change, *p*-adj, and read counts of the DAVID clustered down-modulated genes novel to the 40 min. exposure. Where genes have been duplicated in *Xiphophorus*, information for both copies are presented.

Gene Name	Ensembl ID	*p*-adj.	Fold Change	Avg. Read Count
psma5	ENSXMAT00000004034	5.9E-03	-2.2	2382.1
hp1bp3	ENSXMAT00000017782	8.4E-03	-2.3	1094.8
h2afz	ENSXMAT00000007688	3.9E-03	-2.3	2436.9
tuba1b	ENSXMAT00000003940	3.1E-03	-2.4	3854.5
brip1	ENSXMAT00000005761	9.6E-03	-2.4	328.9
pold1	ENSXMAT00000011809	6.5E-03	-2.4	734.5
smc4	ENSXMAT00000018392	9.0E-04	-2.6	3283.4
ncapd3	ENSXMAT00000005736	1.3E-03	-2.6	1486.2
unga	ENSXMAT00000018321	5.7E-03	-2.6	201.6
fam83d	ENSXMAT00000009629	1.8E-03	-2.6	608.0
ddx11	ENSXMAT00000003969	3.2E-03	-2.6	366.8
cenpo	ENSXMAT00000015198	5.6E-03	-2.6	219.8
nde1	ENSXMAT00000013035	9.5E-03	-2.7	137.3
fanci	ENSXMAT00000000980	6.1E-04	-2.8	521.5
ncapd2	ENSXMAT00000011518	2.4E-04	-2.8	2368.4
kntc1	ENSXMAT00000017710	2.3E-04	-2.9	484.2
e2f3	ENSXMAT00000009710	3.2E-03	-2.9	164.2
rad54l (2 of 2)	ENSXMAT00000006102	3.1E-03	-2.9	130.5
ncapg2	ENSXMAT00000002411	3.7E-04	-3.0	621.0
nuf2	ENSXMAT00000006891	2.3E-04	-3.0	384.4
tk1	ENSXMAT00000000255	2.7E-04	-3.0	343.3
cdc45	ENSXMAT00000014828	2.7E-03	-3.0	854.9
cit (2 of 2)	ENSXMAT00000018396	8.9E-05	-3.1	365.1
kif20ba	ENSXMAT00000004879	2.3E-05	-3.2	558.5
cenpe	ENSXMAT00000010065	1.3E-05	-3.3	547.2
h2afvb	ENSXMAT00000016868	5.1E-03	-3.4	2608.5
foxm1	ENSXMAT00000017715	7.8E-03	-3.5	98.9
rad54b	ENSXMAT00000013190	1.4E-05	-3.5	445.5
fancd2	ENSXMAT00000001648	7.3E-04	-3.7	343.1
spag5	ENSXMAT00000010119	2.1E-06	-3.8	677.5
ncapg	ENSXMAT00000009865	2.2E-06	-3.8	554.1
e2f2	ENSXMAT00000012609	1.4E-04	-3.8	134.6
rad51	ENSXMAT00000000594	1.0E-05	-3.9	262.7
haus3	ENSXMAT00000001754	7.0E-03	-3.9	321.5
haus7	ENSXMAT00000004671	7.9E-04	-3.9	97.3
aspm	ENSXMAT00000000723	5.4E-06	-4.1	791.5

Table 4-10-Continued: Table exhibiting gene name, Ensembl transcript ID, fold change, *p*-adj, and read counts of the DAVID clustered down-modulated genes novel to the 40 min. exposure. Where genes have been duplicated in *Xiphophorus*, information for both copies are presented.

Gene Name	Ensembl ID	*p*-adj.	Fold Change	Avg. Read Count
polq	ENSXMAT00000012655	1.0E-02	-4.2	237.7
fbxo5	ENSXMAT00000017232	3.6E-04	-4.2	83.7
racgap1 (2 of 2)	ENSXMAT00000018543	5.1E-04	-4.2	233.7
chaf1b	ENSXMAT00000004119	4.6E-03	-4.2	464.6
exo1	ENSXMAT00000010548	7.0E-03	-4.8	76.2
ccnf	ENSXMAT00000004757	3.2E-07	-4.8	362.1
ska1	ENSXMAT00000016127	3.0E-07	-5.2	175.9
cep55l	ENSXMAT00000008035	1.2E-04	-5.3	184.6
gsg2	ENSXMAT00000009873	2.8E-04	-5.6	51.8
ccnb2	ENSXMAT00000014334	3.9E-03	-6.1	154.6
spc25	ENSXMAT00000011885	3.2E-07	-34.6	39.0

D) Functional Clusters After 60 min. Exposure

Eighty DE up-modulated 40 min. genes were unique from the overall up-modulated response. Bioinformatic analysis of these genes resulted in the clustering of 14 unique genes into 2 gene ontologies: “epidermis development” and “carboxylic acid catabolic process” (**Table 4-13**).

Sixty-six DE down-modulated 40 min. genes were unique from the overall down-modulated response. Bioinformatic analysis of these genes resulted in the clustering of 19 unique genes into 4 gene ontologies: “response to DNA damage stimulus”, “cell cycle”, “DNA metabolic process” and “actomyosin structure organization” (**Table 4-15**).

Table 4-11: Fourteen of the eighty up-modulated genes novel to the 60 min. exposure clustered into 2 unique GO clusters (p-value < 0.01, list not repeated).

GO ID	Description	p-Value	# Genes	Genes
GO:0008544	epidermis development	4.68E-06	8	DSP, EVPL, FOXQ1, JAG1, LAMC2, PPL, SCEL, TGM1
GO:0046395	carboxylic acid catabolic process	5.36E-05	6	AKR1D1, BCKDK, GLDC, HGD, HPD, PAH

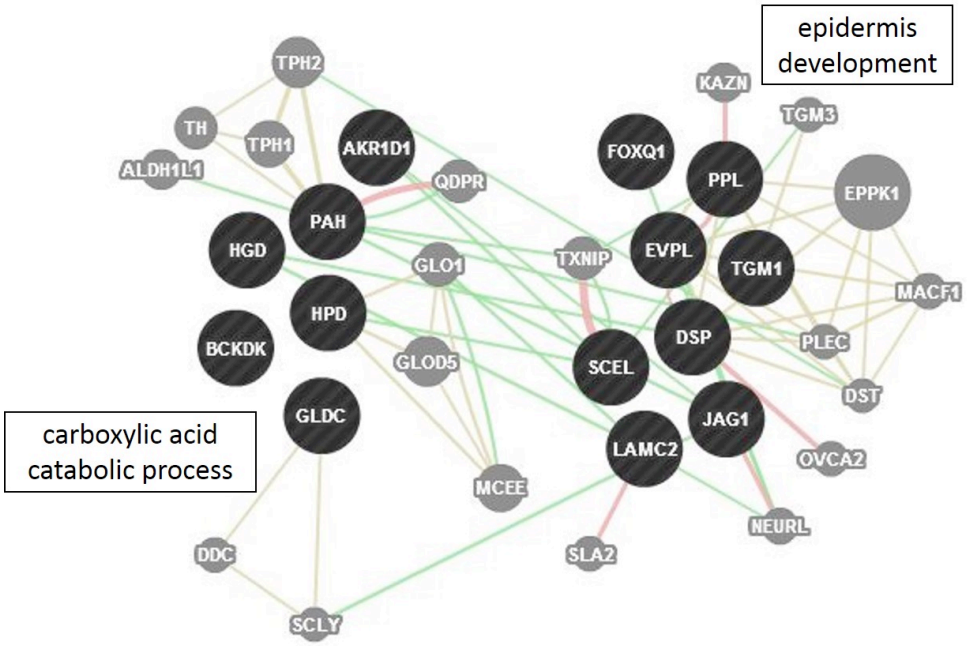

Fig. 4-4: GeneMania network representing 14 DAVID derived 60 min. up-modulated genes unique from the shared up-modulated response to CO. Queried genes are presented as black nodes. Predicted genes are presented as grey nodes. Yellow lines indicate gene products share a protein domain. Red lines indicate a physical interaction between gene products. Green lines indicate a modulation in expression of one gene affects another (i.e. genetic interaction). DAVID derived GO clusters are differentiated by labels.

Table 4-12: Table exhibiting gene name, Ensembl transcript ID, fold change, *p*-adj, and read counts of the DAVID clustered up-modulated genes novel to the 60 min. exposure Where genes have been duplicated in *Xiphophorus*, information for both copies are presented.

Gene Name	Ensembl ID	*p*-adj.	Fold Change	Avg. Read Count
gldc	ENSXMAT00000003064	1.4E-04	2.7	13104.7
akr1d1 (1 of 2)	ENSXMAT00000004428	1.9E-03	2.6	195.9
foxq1a	ENSXMAT00000019885	1.2E-03	2.6	716.8
bckdk	ENSXMAT00000008840	1.7E-03	2.5	8045.8
lamc2	ENSXMAT00000011334	5.9E-04	2.5	7084.1
evpla (2 of 2)	ENSXMAT00000006115	8.3E-04	2.5	13814.1
ppl	ENSXMAT00000015036	8.7E-04	2.4	19287.4
scel	ENSXMAT00000011194	1.9E-03	2.4	2493.7
tgm1	ENSXMAT00000012731	1.2E-03	2.3	1024.8
hgd	ENSXMAT00000019083	7.9E-04	2.3	1622.9
hpdb	ENSXMAT00000015288	5.4E-03	2.2	3239.5
evplb	ENSXMAT00000008332	3.0E-03	2.2	14102.9
dspa	ENSXMAT00000016895	1.9E-03	2.2	32805.7
jag1b	ENSXMAT00000006401	1.7E-03	2.1	10498.6
pah	ENSXMAT00000017348	1.9E-03	2.1	4381.7

Table 4-13: Nineteen of the sixty-six down-modulated genes novel to the 60 min. exposure clustered into 4 unique GO clusters (*p*-value < 0.01, list not repeated).

GO ID	Description	*p*-Value	# Genes	Genes
GO:0006974	response to DNA damage stimulus	1.9E-05	9	ALKBH2, ATM, BARD1, CRY1, MDC1, MSH6, NEIL3, RECQL4, TIMELESS
GO:0007049	cell cycle	2.1E-05	12	ATM, BARD1, CENPE, FBXO5, MDC1, MSH6, NUF2, RACGAP1, SKA1, SPC25, SUV39H1, TIMELESS
GO:0006259	DNA metabolic process	1.6E-04	9	ALKBH2, ATM, BARD1, CRY1, IGFBP4, MDC1, MSH6, NEIL3, RECQL4
GO:0031032	actomyosin structure organization	3.5E-03	3	RACGAP1, TMOD1, TNNT2

Table 4-14: Table exhibiting gene name, Ensembl transcript ID, fold change, *p*-adj, and read counts of the DAVID clustered 60 min. down-modulated genes. Where genes have been duplicated in *Xiphophorus*, information for both copies are presented.

Gene Name	Ensembl ID	*p*-adj.	Fold Change	Avg. Read Count
igfbp4	ENSXMAT00000018240	4.5E-03	-2.1	1427.2
mdc1	ENSXMAT00000011013	9.0E-03	-2.1	724.7
msh6	ENSXMAT00000011028	5.8E-03	-2.1	1306.6
cry1b	ENSXMAT00000001763	1.1E-03	-2.3	1153.6
nuf2	ENSXMAT00000006891	6.8E-03	-2.3	387.8
timeless	ENSXMAT00000003313	5.7E-03	-2.3	439.9
tnnt2d (1 of 2)	ENSXMAT00000008992	2.0E-03	-2.3	1041.5
tnnt2d (2 of 2)	ENSXMAT00000017101	3.7E-03	-2.3	2727.7
cenpe	ENSXMAT00000010065	4.3E-04	-2.5	543.8
recql4	ENSXMAT00000015382	6.0E-03	-2.5	222.6
ska1	ENSXMAT00000016127	8.0E-03	-2.5	192.4
bard1	ENSXMAT00000016055	9.1E-03	-2.6	104.5
amt	ENSXMAT00000019396	5.8E-04	-2.8	216.6
neil3	ENSXMAT00000002242	6.6E-03	-2.8	95.3
tmod1	ENSXMAT00000006124	3.4E-03	-2.8	143.4
fbxo5	ENSXMAT00000017232	5.7E-03	-3.0	82.8
racgap1 (2 of 2)	ENSXMAT00000018543	6.8E-03	-3.0	232.6
suv39h1a	ENSXMAT00000012911	6.7E-03	-3.2	332.7
alkbh2	ENSXMAT00000018313	6.9E-03	-4.9	37.6
spc25	ENSXMAT00000011885	5.0E-03	-6.1	41.1

E) Functional Clusters After 80 min. Exposure

Eighty DE up-modulated 80 min. genes were unique from the overall up-modulated response. Bioinformatic analysis of this gene set resulted in the clustering of 7 unique genes into 2 gene ontologies: “carboxylic acid catabolic process” and “lipid catabolic process” (**Table 4-17**). These seven genes did not show associations to each other by either shared protein domains, physical interactions or genetic interactions. Fourteen down-modulated 80 min. genes were unique from the overall down-modulated response (**Table 4-19**). These 14 genes did not cluster through DAVID bioinformatic

analysis, nor did they show associations to each other by either shared protein domains, physical interactions or genetic interactions using GeneMania.

Table 4-15: Eight of the nineteen up-modulated genes novel to the 80 min. exposure clustered into 2 unique GO clusters (*p*-value < 0.01, list not repeated).

GO ID	Description	*p*-Value	# Genes	Genes
GO:0046395	carboxylic acid catabolic process	1.22E-03	4	BCKDK, CPT1B, HGD, HPD
GO:0016042	lipid catabolic process	4.30E-03	4	CPT1B, NCEH1, PLCD4,LPL

Table 4-16: Table exhibiting the up-modulated genes novel to the 80 min. exposure, ensembl transcript ID, fold change, *p*-adj, and read counts of the 80 min. up-modulated genes.

Gene Name	Ensembl ID	*p*-adj.	Fold Change	Avg. Read Count
plcd4a	ENSXMAT00000018873	3.1E-04	17.7	91.0
cpt1b	ENSXMAT00000004684	3.5E-07	4.4	382.4
lpl	ENSXMAT00000003462	2.0E-08	4.3	6643.7
nceh1b	ENSXMAT00000004610	1.1E-05	3.6	760.7
bckdk	ENSXMAT00000008840	3.6E-04	2.8	9192.5
hpdb	ENSXMAT00000015288	9.6E-04	2.4	3612.4
hgd	ENSXMAT00000019083	2.4E-03	2.3	1745.8

Table 4-17: Table exhibiting gene name, Ensembl transcript ID, fold change, *p*-adj, and read counts of the 14 down-modulated genes novel to the 80 min. exposure. Where genes have been duplicated in *Xiphophorus*, information for both copies are presented.

Gene Name	Ensembl ID	Description	*p*-adj.	Fold Change	Avg. Read Count
fkbp7	ENSXMAT00000005901	FK506 binding protein 7	5.6E-03	-2.3	958.5
cenpe	ENSXMAT00000010065	centromere protein E	3.6E-03	-2.5	573.6
rhcga	ENSXMAT00000014051	Rhesus blood group, C glycoprotein a	5.3E-03	-2.5	1774.0
wars	ENSXMAT00000007754	tryptophanyl-tRNA synthetase	4.7E-03	-2.5	1105.1
uncharacterized	ENSXMAT00000004025	Uncharacterized protein	1.2E-03	-2.6	576.4
uncharacterized	ENSXMAT00000004562	Uncharacterized protein	1.3E-03	-2.6	541.1
cdt1	ENSXMAT00000015029	chromatin licensing and DNA replication factor 1	7.0E-03	-2.8	169.8
dot1l	ENSXMAT00000012900	DOT1-like, histone H3 methyltransferase (S. cerevisiae)	2.2E-03	-2.8	1780.5
pcsk9	ENSXMAT00000011154	proprotein convertase subtilisin/kexin type 9	7.9E-03	-2.8	196.2
asns	ENSXMAT00000016921	asparagine synthetase	3.7E-04	-3.0	914.3
aspm	ENSXMAT00000000723	asp (abnormal spindle)-like, microcephaly associated (Drosophila)	2.0E-04	-3.0	818.3
znf367	ENSXMAT00000016047	zinc finger protein 367	3.1E-03	-3.0	138.2
uncharacterized	ENSXMAT00000005291	Uncharacterized protein	9.5E-04	-3.2	154.0
alkbh2	ENSXMAT00000018313	alkB, alkylation repair homolog 2 (E. coli)	7.5E-03	-4.9	39.3

Discussion

Within the shared up-modulated response, all 6 genes associated with circadian rhythm process (**Table 4-1**) are reported to help establish and maintain rhythmic expression of cellular processes that occur in vertebrates over an approximate 24 hr cycle (i.e. circadian rhythm) (Wilsbacher and Takahashi, 1998; Reppert and Weaver, 2002). The products of *tln2* and *sptbn4* are involved in maintenance of cell-cell junctions (Bennet, 1990; Praekelt *et al.* 2012). GeneMania visualization of the overall up-modulated gene set revealed shared protein domains and various physical interactions among the rhythmic process associated genes and among the cytoskeletal anchoring associated genes. There were no network associated genes between these two clusters.

Up-modulation of circadian-rhythm associated genes, in particular *cry2*, and phosphorylation indicate light dependent responses were induced in *Xiphophorus* skin. Exposure to light is well known to induce transcriptional activity of some *cry* genes (Oliveri *et al.*, 2014). Cry proteins are both a product and transcriptional repressor of the circadian rhythm associated heterodimer clock/arntl (also known as bmal1) (Reppert and Weaver, 2002; Oliveri *et al.*, 2014). Activity of the clock/arntl heterodimer, and *per* and *cry* gene expression are associated with various non-circadian processes such as cell cycle regulation and metabolism (Fontaine *et al.*, 2003; Takahashi *et al*., 2008). Phosphorylation of circadian-rhythmic genes aids in resetting the molecular circadian clock (Doi *et al*., 2004; Virshup *et al.*, 2007).

Cell-cell adhesion is important in maintenance of tissue organization and structure over an extracellular matrix (ECM) (e.g. collagen, elastic fibers and the basement membrane) (Uitto *et al.*, 1989; Baker and Garrod, 1993; Vasioukhin *et al.*, 2000). The

actin cytoskeleton of cells cooperates with adhesive forces (e.g. focal adhesion, a type of adhesion cells make with the ECM) to maintain either cell-cell adhesions or cell-ECM adhesions (Gumbiner, 1996). Disruption of cell-ECM interactions has been shown to induce apoptosis in cultured cell lines (Frisch and Francis, 1994; Grossman, 2002). Therefore up-regulation of genes involved in cell-cell adhesion could indicate exposure to CO promotes either cell-cell adhesion/cell-ECM adhesion in fish skin. Cell-cell adhesion is reportedly involved in the cellular inflammatory response elicited by tissue injury (Eming *et al.*, 2007). In this response, cell-cell adhesion is utilized in white blood cell migration to the site of injury (Eming *et al.*, 2007). Inflammation induced by visible light exposure (400-700 nm) *in vivo* and in cultured skin cells (Dupont *et al.*, 2013). It is plausible exposure to CO at the various doses elicits a similar inflammatory response in *Xiphophorus* skin.

Within the set of overall shared down-modulated genes the largest cluster is associated with cell cycle progression. Sixty-nine genes within the cell cycle cluster overlapped with 12 other functional clusters. Twenty-eight genes from this subset were related to one or more cell cycle genes by shared protein domain, possibly implicating a shared function. The products of these 28 genes are reported to contribute to proper progression of different phases of the cell cycle and were represented within 6 down-modulated functional categories:

Chromosome segregation/microtubule-based process: Aurora kinase a and b (aurka/aurkb), polo-like kinase 1 (plk1) and tyrosine kinase ttk help to maintain proper spindle formation and chromosome segregation during mitosis (Golsteyn *et al.*, 1995; Andrews *et al*., 2003; Malumbres & Barbacid, 2007). The product of *bub1b* is reported to

assist in chromatid adhesion via centromeres during mitosis (Tange *et al.,* 2004), while bub1 protein is required for the cell to detect spindle damage and mitotic progression (Taylor and McKeon, 1997; Davenport *et al*., 1998). Transcription factors E2F7 and E2F8 are suspected to prevent abnormal nuclear division (i.e. karyokinesis) during mitosis (Lammens *et al*., 2009).

DNA metabolic process/protein-DNA complex associated mcm2 and mcm6 are subunits of the mcm-complex, which has a role in the initiation of DNA synthesis (Lei and Tye, 2001). The *cdc7* product phosphorylates this mcm-complex (Cho *et al.*, 2006). Additional DNA metabolic associated genes include *rpa1, hells* and *ercc6l* which each have varying roles in DNA repair and replication (Troelstra *et al.*, 1993; reviewed by Geiman *et al.*, 1998; Haring *et al.*, 2008).

Cyclin proteins (ccna2, ccnb1, ccnb3) and cyclin dependent kinases (cdk1, cdk2) are associated with the **phosphoinositide kinase-mediated signaling/protein amino acid phosphorylation** clusters. Cyclins form active complexes with cyclin dependent kinases to initiate phosphorylation activity of the cdks (Doree and Galas, 1994). These complexes aid in progression of the cell cycle phase transitions (Sherr, 1993; Hartwell and Kastan, 1994, Walker, 2001). *Pbk*, *pkmyt1* are kinase genes involved in cell cycle progression via regulation of cell cycle regulator *cdc2* and the tumor suppressor gene *pten* (Gaudet *et al.*, 2000; Dephoure *et al*., 2008). Kinesin superfamily proteins (KIF2C, C1, 15, 18A, 22 and 23) are associated with the **microtubule-based processes** cluster. These proteins aid in transport of membranous organelles, protein complexes and mRNA transcripts (Hirokawa and Takemura, 2004).

Forty-two of the remaining cell cycle associated genes did not share a protein domain, however did appear in at least one of ten other clusters of down-modulated genes. Only one of the clusters can be specifically associated with the M-phase of the cell cycle (chromosome segregation), while the other functions can be associated with either the M or the S-phase (DNA metabolic process, DNA packaging, microtubule based process, phosphoinositide-mediated signaling, protein-DNA complex assembly, negative regulation of cellular component organization and cellular macromolecular complex subunit organization).

Two clusters ("cell proliferation" and "DNA damage stimulus") were not associated specifically with either the M or the S-phase of the cell cycle. Genes within the cell proliferation cluster that did not share a protein domain with another gene included *mki67*, *dlgap5*, *racgap1*, *tacc3* and *tpx2*. The products of these genes have been reported to aid in progression of each phase (G_0 withstanding) of the cell cycle (Schlozen and Gerdes, 2000), aid in proper mitotic spindle and kinetochore assembly (Hirose *et al.,* 2001; Bayliss *et al.,* 2003; Wilde, 2006) and in proper chromosome alignment during mitosis (Schneider *et al*, 2007). Given that proliferation of a cell includes both growth and cell division, it is understandable that genes within this category would be associated with specific phases of the cell cycle, in this case the M-phase.

Genes within the DNA damage stimulus cluster that did not share a protein domain with another cell cycle associated gene included *chaf1a*, *clspn*, *gtse1*, *pttg* and *rad52*. While extensive exposure (20 hrs) of transformed mouse cultured cells to cool white fluorescent light has been reported to induce DNA damage (Gantt *et al.*, 1978), a literature search reveals there are not many, if any, studies regarding the possible DNA

damaging effects of CO light. These particular genes are reportedly involved in regulation of cell proliferation and differentiation (Zhang *et al*., 1999; Barbieri *et al*., 2013), regulation of cell migration via microtubule assembly (Scloz *et al*., 2000), regulation of the cell cycle regulator, *chek1* (Liu *et al*., 2012) and homologous recombination and repair (Lisby *et al*., 2001). All of these functions can be associated with general cell cycle progression, thus it is understandable why they are shared between the cell cycle cluster and the DNA damage stimulus cluster. While down-modulation of genes related to DNA repair may implicate CO does not induce DNA damage, it is more indicative of the S-phase suppression, during which DNA repair occurs (Bartek *et al.*, 2004).

Physical interactions and association of shared protein domains among the various cell cycle associated genes have been visualized via gene networking. Eight of the cell cycle genes (i.e. *anln*, *cdca3*, *esco2*, *mtbp*, *nusap1*, *pole*, *rbbp8*, *sass6*, *zwilch*) do not associate with other cell cycle genes by either protein-protein interaction (i.e. physical interaction) or via shared protein domains. Down-modulation of these and the previously discussed genes related to either mitosis (M-phase) or DNA replication (S-phase) indicate exposure to CO either does not induce or promote cell division or DNA replication, or it actively suppresses these phases.

Tamai *et al.* (2012) report a similar suppressive response in cultured zebrafish cells after constant exposure to general fluorescent light. In this experiment several lines of cultured zebrafish fibroblasts were exposed to either a light:dark (LD) cycle of 12:12 hrs, or a cycle where the cells were exposed to constant light (LL), for 6-7 days. Cells kept under the LL cycle exhibited arrhythmic cell division and suppressed cell

proliferation. Tamai *et al.* (2012) attributed this result, in part, to overexpression of zebrafish *cry1a* activity by the constant fluorescent light exposure. A previous experiment from these researchers showed zebrafish cry1a protein disrupts activity of the clock/arntl heterodimer, therefore preventing proper expression of *per* and *cry* genes (Tamai *et al.,* 2007). Tamai *et al.* (2012) supported clock-dependent mitosis by showing double negative *clock* mutant zebrafish cells exhibited reduced activity of *cyclin B1, cyclin B2* and *cdc2*, genes associated with progression of mitosis.

Though our data presented show mitosis associated genes exhibit down-modulation and *clock* as up-modulated in response to CO exposure, this may be attributed to a duplication of genes within zebrafish. All teleost have undergone a genome duplication within the course of their evolutionary timeline (Glasauer and Neuhauss, 2013). Thus, a number of genes have multiple copies that vary in functionality (e.g. *cry*; Kobayashi *et al.,* 2000). Kobayashi *et al.* (2000) describes the range in functionality of 6 different zebrafish *cry* genes, some of which have not retained transcriptional repression activity of the clock/arntl heterodimer. Thus, the copy of clock (*clock1a*) Tamai *et al.* (2012) identified as influencing mitotic progression may be may be influenced by the copy of *cry* that is down-modulated in our data (*cry1b*), rather than the copy that is up-modulated (*cry2a*). Zebrafish also have multiple copies of the *clock* gene (Vatine *et al.,* 2011) thus, it is also plausible the copy of *clock* from the Tamai *et al.* (2012) study may be a different copy in *Xiphophorus*. Alternatively, *clock* expression *in vivo* is concomitantly regulated by an additional biological mechanism that is likely to differ in the intact whole animal compared to transformed cultured cells.

Once the overall up and down-modulated shared response was functionally assessed, the genes at each exposure that were not found in the overall shared set (i.e. novel) were then functionally assessed. Four novel up-modulated 20 min. genes exhibited clustering specifically with "rhythmic process". The genes within this 20 min. cluster are unique from the circadian-rhythmic process associated genes in the overall shared set. Only *nfil3* (also known as *rev-erb*α) has been reported to help establish the circadian rhythm of a process (Mertelot *et al.*, 2009). Instead of directly contributing to establishment of the molecular circadian cycle these genes have been reported to show rhythmic activity in human cultured cells (Arjona *et al.,* 2004) and in rodent tissues (Falvey *et al*. 1995; Sekiguchi *et al.* 2004; Lauriola *et al.*, 2014).

Novel 20 min. up-modulated "phosphorylation" and "transmembrane receptor protein tyrosine kinase signaling pathway" clusters are primarily composed of genes encoding for kinases. There is a considerable amount of literature showing involvement of these genes in cellular signaling pathways not associated with the M-phase kinases discussed in the overall down-modulated gene set (Tavakkol *et al.*, 1992; Schlessinger, 2000; Shirakata *et al*., 2000; Machius *et al.*, 2001; Song *et al.*, 2004; Tsuchida *et al.*, 2004; reviewed by Kitano-Takahashi *et al.* 2007; Hui *et al.*, 2008; Bradley and Koleske, 2009; Cahill *et al.*, 2009; Rose *et al.*, 2009; Blind *et al.*, 2012; Yang *et al.* 2012). Up-modulation of these genes may act as signaling precursors for novel clusters found in gene sets of our later exposures.

Novel 20 min. down-modulated genes clustered into many of the same functional sets as observed in the overall down-modulated shared set. The genes within these clusters also exhibited overlap between clusters. "Chromosome organization" was a

novel function not found among the list of functional clusters from the shared response, but chromosome organization could be attributed with preparation of chromatin for the mitotic phase. Novel down-modulated 40 and 60 min. genes all clustered into cell cycle, mitosis or DNA synthesis associated functions. Down-modulation of genes involved in these processes in both the overall shared response and at individual exposures suggests any of these doses may serve to suppress cell cycle and related functions in *Xiphophorus* male skin.

The lack of clustering among the novel DE down-modulated 80 min. genes can be attributed to the small fraction (16%) of unique genes at that exposure (**Table 3-3**). Four (cenpe, cdt1, alkbh2, aspm) of the novel fourteen down-modulated 80 min. genes appear in clusters of various other exposures and are involved in chromosome alignment (Ditchfield *et al*., 2003), DNA replication (Nishitani *et al.*, 1999), repair of alkylated DNA bases (Nay *et al.*, 2012) and mitotic spindle formation (Fish *et al*., 2006). Down-modulation of these genes suggests suppression of the M and S-phase persists after prolonged exposure. The remaining 8 genes have been characterized in other vertebrates and are reportedly involved in various processes such as ammonia secretion (Weiner and Verlander, 2014), invasive cell migration (Jain *et al.,* 2014), cholesterol homeostasis (Abifadel *et al.*, 2003), amino acid and protein synthesis (Doublié, *et al*., 1995; Siu *et al.* 2002), and transcriptional regulation (Park *et al.*, 1992; Steger *et al.*, 2008).

Down-modulation of significant DE 80 min. genes, as discussed in chapter 3, could be reflective of an adaptation of the skin to the CO exposure after its dark cycle. Down-modulation of genes associated with amino acid/ protein synthesis and transcriptional regulation could support this speculation. Once the tissue has adapted to a

new stimuli, the need for extraneous proteins dwindles. Thus, transcription must be negatively regulated for expression to level. If the speculation that *Xiphophorus* skin has adapted to CO exposure after 80 min. is assumed, down-modulation of *rhcga*, a gene involved in ammonia secretion (Wright and Wood, 2009), could reflect adaptation of the tissue to CO exposure as ammonia secretion is a normal function in fish skin (Randall and Wright, 1987).

Znf367 is reported to contribute to the invasive migration when overexpressed in endocrine linked cancers (Jain *et al*., 2014). Normal activity of this gene could involve regulation of hormone levels. However, studies of this gene and its product are limited in the literature so this speculation is not well supported. In regard to the down-modulation of a gene involved in cholesterol homeostasis, one 80 min. up-modulated genes (*nceh1*) is also involved in cholesterol homeostasis. Whereas *nceh1* has shown specific involvement in cholesterol transporting macrophages (Vainio and Ikonen, 2003; Sekiya *et al.*, 2011), dysregulation of proper *pcsk9* activity affects production of *narc1* (Abifadel *et al.*, 2003) that is associated with hypercholesterolemia, a disease where excessive levels of cholesterol are retained in the bloodstream. Given this information and data exhibiting opposite modulations, it is possible *nceh1* and *pcsk9* play opposing roles in the cholesterol transport system.

Novel up-modulated 40 min. genes exhibited clustering related to phosphorylation, similar to the overall shared response. The “muscle development” cluster is unique and may be attributed to muscle RNA contamination during the dissection of the skin. These genes are reported to have roles in striated muscle cells of land vertebrates involving fatty acid oxidation (Bruce *et al*., 2008), T-Cell receptor

mediated signal transduction (Swanson *et al*., 1998), reorganization of the actin cytoskeleton (reviewed by Crowley *et al.*, 2009), morphogenesis (Lidral *et al.*, 1998), and attachment of filaments (Bang *et al.*, 2001). Gene network interactions exhibit more genetic interactions between queried genes than physical interactions. This could be attributed to the phosphorylation related genes, which act in a variety of signaling pathways, as discussed in the novel 20 min. clusters.

Novel up-modulated 60 min. genes were segregated into 2 unique clusters: "epidermis development" and "carboxylic acid metabolic process". Genes within the epidermis development cluster are involved in developmental processes such as epithelial cell-cell adhesion (Bornslaeger *et al.*, 1996; Vasioukhin *et al.*, 2001), skin cell morphology and maturation (Nickoloff *et al.*, 2002; Eckert *et al.*, 2005; Feuerborn *et al.*, 2011), maintenance of the basement membrane, a membrane which separates epithelial cells from mesenchyme cells (Fleischmajer *et al.*, 1998) and development of precursory skin cells (Champliaud *et al.*, 2000). Genes within the carboxylic acid metabolic process cluster are reported to be involved in bile acid synthesis (Lee *et al.*, 2009), catabolism of branched chain amino acids and amino acids containing aromatic rings (reviewed by Machius *et al.*, 2001; Moran, 2005; Phornphutkul *et al.*, 2011; Flydal and Martinez, 2013) and NADH production (Kikuchi *et al.*, 2008). That these novel up-modulated clusters are observed at 60 min. of exposure, but not 20, 40 or 80 min. suggest this dose of CO is optimal for tissue development and organization. Increased expression of genes involved in catabolic processes might reflect an increased need for energy in the tissue.

Novel up-modulated 80 min. genes were clustered into two functional categories that were unique from the shared response. The "carboxylic acid catabolic process"

cluster contained genes shared with the same cluster exhibited at 60 min. implicating it is possibly a response shared with the 60 min. exposure. The "lipid catabolic process" cluster was a novel cluster. Lipid catabolic clustered genes have shown functions in cholesterol transport (Sekiya *et al.*, 2011), lipid catabolism (Eckel, 1989) and fatty acid oxidation (Bruce *et al.*, 2008) and second messenger signaling (Rhee, 2001) when expressed. In mammals, fatty acids are incorporated into and used by epithelial cells for energy, lipid bilayer formation and signaling (Lin and Khnykin, 2014). The presence of genes associated with cholesterol, lipid and fatty acid catabolism could be a persisting response of the up-modulated expression of skin development genes observed at the 60 min. exposure.

Validations.

qRT-PCR

Quantitative real time-PCR was used to verify bioinformatic calculated fold changes in gene expression of a subset of 5 CO modulated genes, 3 of which exhibited ± 2 fold change. The genes chosen for this analysis include the M-phase associated gene *cenp-f*, the circadian-rhythmic process associated gene *per1b*, and the light inducible gene *cpd* photolyase. In CO exposed skin, the expression of *cenp-f* was significantly down-modulated (-2 fold, p-adj < 0.01) in all exposures in RNA-Seq derived data, but only significantly down-modulated at 40 and 80 min. of exposure in qRT-PCR verification (**Fig. 5-1**). *Per1b* expression was significantly down-modulated (-2 fold, p-adj < 0.01) in all exposures by RNA-Seq derived data, and in all exposures of in qRT-PCR verification (**Fig. 5-2**). *Cpd* expression in response to cool white fluorescent light has been previously characterized in *Xiphophorus* skin (Walter *et al.*, 2014), thus it was

used to validate a light-inducible response. *Cpd* expression was up-modulated 1.58 fold or greater in RNA-Seq derived data, and 1.73 or greater in qRT-PCR verification (**Fig. 5-3**). *Cpd* was expressed with a *p*-adj. value ≤ 0.25, 0.02, 0.02, 0.02 at 20, 40, 60 and 80 min. of exposure, respectively.

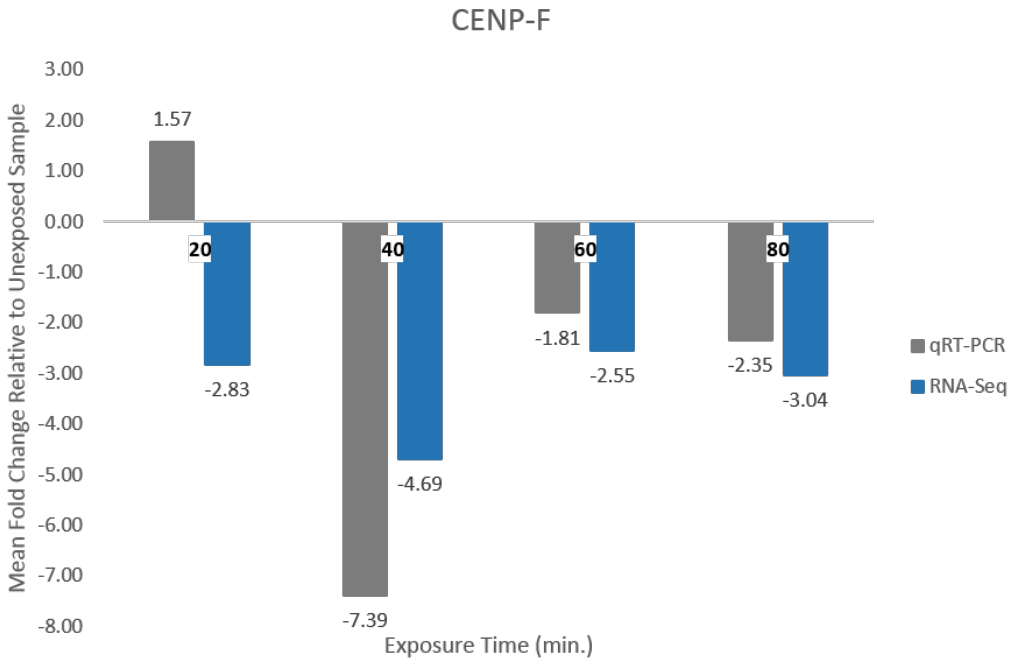

Fig. 5-1: Table exhibiting comparisons of qRT-PCR quantified fold change (grey) versus RNA-Seq quantified data (blue) for the *cenpf* transcript at various CO doses.

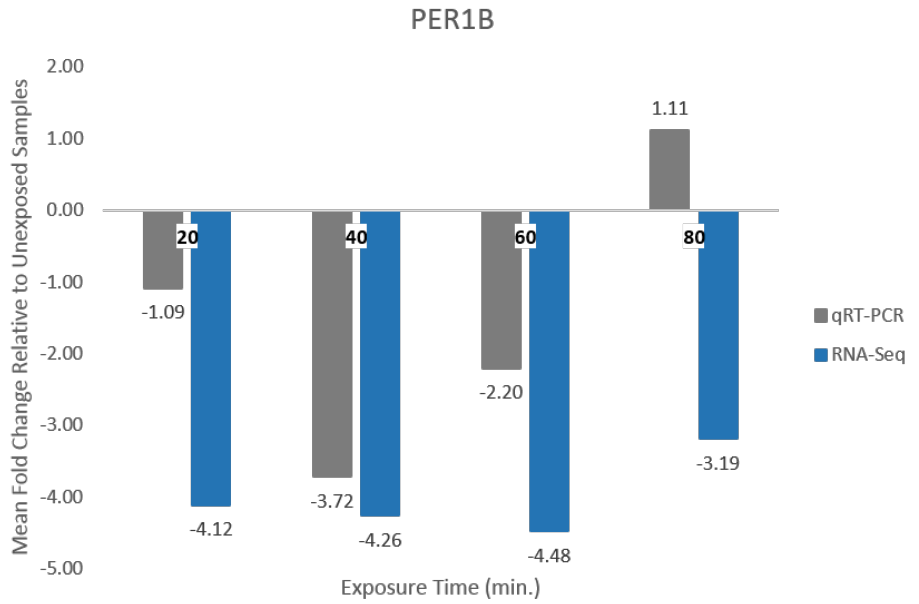

Fig. 5-2: Table exhibiting comparisons of qRT-PCR quantified fold change (grey) versus RNA-Seq quantified data (blue) for the *per1b* transcript at various CO doses.

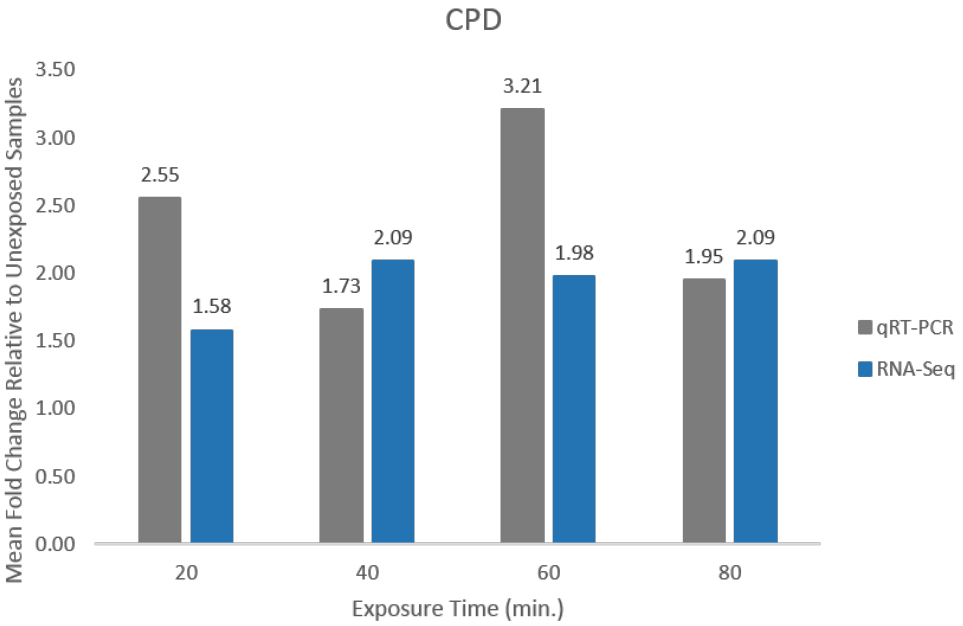

Fig. 5-3: Table exhibiting comparisons of qRT-PCR quantified fold change (grey) versus RNA-Seq quantified data (blue) for the light-inducible *CPD* transcript at various CO doses.

NanoString

NanoString technology was used to independently verify bioinformatic calculated fold change in gene expression of a subset of CO modulated genes. Fourteen of nineteen probes tested in NanoString were significantly modulated (± 2 fold change, *p*-adj < 0.01) in the overall shared RNA-Seq derived data set (grey gene name, **Table 5-1**). The remaining were significantly modulated (± 2 fold change, *p*-adj < 0.01) at individually designated exposures (blue text, **Table 5-1**).

Table 5-1: Table exhibiting gene name, Ensembl transcript ID and fold change associated with 19 gene probes used in NanoString analysis compared to data generated by bioinformatic analysis of the RNA-Seq data. Fourteen of the nineteen probes match to the gene set of the overall shared response (grey gene name, white text). The remaining 5 gene probes were significant (± 2 fold change, *p*-adj < 0.01) in an individual exposures (blue text). Asterisked exposure indicates a single biological sample was sent for analysis.

		NanoString			RNA-Seq		
Gene Name	Ensembl ID	20 min.	60 min.*	80 min	20 min.	60 min.	80 min
klhl38b	ENSXMAT00000008690	2.07	1.96	3.86	**17.02**	11.65	35.02
clock	ENSXMAT00000017010	2.22	2.30	1.72	3.37	3.02	2.17
dnah7	ENSXMAT00000007381	1.06	1.56	1.13	3.35	3.16	2.72
cry2a	ENSXMAT00000009327	1.43	1.38	1.30	2.89	2.94	2.08
ppp1r27	ENSXMAT00000018069	-2.72	-5.42	-1.71	-2.69	1.12	**1.09**
ccnf	ENSXMAT00000004757	-1.00	1.11	1.21	**-2.81**	-2.53	-2.42
spc25	ENSXMAT00000011885	-1.12	1.11	-1.41	-3.16	**-6.03**	-2.63
fggy	ENSXMAT00000018361	-1.19	1.00	1.10	-3.23	-2.68	-2.28
raver1	ENSXMAT00000000218	-1.09	-1.11	1.05	-3.34	-4.88	-3.74
kifc1	ENSXMAT00000016886	1.11	1.31	1.26	-3.49	-3.11	-3.00
arhgap19	ENSXMAT00000014517	-1.07	-1.06	1.06	-3.50	-2.59	-3.05
numa1	ENSXMAT00000011193	1.01	1.07	1.12	-3.58	-3.21	-2.99
cdk1	ENSXMAT00000014787	1.04	1.23	1.19	-3.67	-3.19	-2.92
mad2l1	ENSXMAT00000017587	-1.01	1.11	1.13	-3.68	-3.08	-2.53

Table 5-1-Continued: Table exhibiting gene name, Ensembl transcript ID and fold change associated with 19 gene probes used in NanoString analysis compared to data generated by bioinformatic analysis of the RNA-Seq data. Fourteen of the nineteen probes match to the gene set of the overall shared response (grey gene name, white text). The remaining 5 gene probes were significant (± 2 fold change, *p*-adj < 0.01) in an individual exposures (blue text). Asterisked exposure indicates a single biological sample was sent for analysis.

		NanoString			RNA-Seq		
Gene Name	Ensembl ID	20 min.	60 min.*	80 min	20 min.	60 min.	80 min
bhlhe40 (1 of 2)	ENSXMAT00000002257	-3.24	-2.72	-2.02	**-3.99**	-3.68	-2.28
parpbp	ENSXMAT00000017412	1.41	1.32	1.37	-4.13	-3.76	-3.56
kpna2	ENSXMAT00000008371	1.16	1.25	1.31	-4.19	-4.48	-3.82
pif1	ENSXMAT00000003968	-1.20	1.00	-1.04	-4.46	-4.25	-3.23
cdca7a	ENSXMAT00000005334	-2.10	-1.29	-1.24	-8.53	-4.74	-4.58

CHAPTER V

SUMMARY & CONCLUSIONS

Previous experiments and health reports regarding the possible impact of "cool white" fluorescent lights (4,100 K) on biological functions and overall health of an organism led us to question whether exposure to full spectrum fluorescent light (10,000 K), advertised to mimic the full spectrum of sunlight, might elicit a different response at the molecular genetic level. Thus, we utilized a classic vertebrate model *Xiphphorus maculatus* Jp 163 B to investigate this possibility. Exposure of this model organism to full spectrum fluorescent light and subsequent analysis of RNA-Seq data from their exposed skin revealed DE down-modulation of over half the significantly modulated genes in the gene set for each dose.

Various comparisons among the DE gene sets from various exposure times, revealed the majority of these down-modulated genes were shared among the exposures. While the number of up-modulated DE genes were limited in each exposure set, these genes exhibited higher fractions of unique genes indicating each of the various exposures prompted a novel up-modulated response. Functional clustering of the overall genetic response (i.e. genes shared between 20, 40, 60 min. and with the 80 min. exposure) and of genes from each exposure set that were unique from this overall shared set has given an insight into the shared response to CO and the unique genetic response for individual CO exposures.

Six genes clustered by circadian rhythm process in the overall shared up-modulated genes. Up-modulation of two of these genes has been described as a light-responsive expression pattern. This suggests a light dependent response was induced by

CO exposures in *Xiphophorus* skin. Up-modulated clusters associated with signaling (phosphorylation) and cell-cell adhesion in epithelial cells also suggest exposure to CO helps perpetuate normal maintenance of cellular processes and structural integrity of the tissue *in vivo*. The overall shared down-modulated response was primarily composed of genes that were associated with stalling mitosis and DNA-synthesis.

Up-modulation of genes involved in maintenance of skin structure and the persistent down-modulation of genes involved in cell cycle processes, specifically those associated with mitosis and DNA synthesis, suggests exposure to CO either induces stalls mitosis and alters the G_1-S checkpoint. While not necessarily the determining factor, one clue pointing to G_1 phase effects are proliferation markers, such as mki-67. The mki-67 protein is generally used as a proliferation marker (Schlozen and Gerdes, 2000). In cells progressing through the cell cycle, presence of mki-67 protein is observed at all but the G_0 phase (Schlozen and Gerdes, 2000).

Skin fibroblasts are generally arrested in the G_0 phase unless stimulated to enter the cell cycle (Cooper, 2000). In general, once entering into G_1 phase, nutrient and protein requirements are necessary for the cell to progress to the S-phase. To support the speculation that CO exposure induces stalling of mitotic progression in the G_1 phase, various growth factors in skin cells (i.e. ereg, ghr, igf1r, tgfbr3 and fgf23) are up-modulated at 20, 40 and 60 min. of CO exposure. Tgf-β genes and igf1 genes are known to be involved in nutrient signaling (Foster *et al.*, 2011); cells must meet proper nutrient requirements before proceeding into the S-phase of the cell cycle. Ghr and ereg have exhibited involvement in growth signaling in human skin cells (Tavvakol *et al.*, 1992; Shirakata *et al.*, 2000), while fgf23 has shown involvement in vitamin-D production, the

lack of which has been shown to contribute to poor epidermal cell differentiation in mice (Xie *et al*., 2002).

The time for a complete round of the cell cycle varies depending on the cell type, several studies evaluating the duration of the cell cycle in both primary explants and transformed human epidermal cells have reported each phase of the epithelial cell cycle can take a number of hours (Flaxman and Chopra, 1972; van Erp *et al.*, 1996). All layers of fish skin, unlike human skin, are living and metabolically active that must be able to deal with the challenges of an aquatic environment (e.g. aquatic bacteria, thermal regulation, osmosis) (Esteban, 2012). A relatively rapid proliferation rate would allow fish skin to reduce the time an open wound is exposed to the environment. Thus, it is plausible the duration for which these exposures were performed provide insight to the beginning of the G_1 phase versus cells waiting in a dormant phase. The reduction in number of both DE up and down-modulated genes at 80 min. of exposure might reflect the shift from G_1 into the subsequent S-phase.

Among the novel responses of individual exposures, exhibition of up-modulated genes associated with tissue structure and catabolic processes suggest higher doses of CO (i.e. $\geq$ 60 min.) may help to maintain the integrity of fish skin and promote energy producing processes. Given the information taken from these data sets, current and future experiments may include an analysis of female *X. maculatus* Jp 163 B RNA-Seq data to determine if this responses in this study are sex specific, an RNA-Seq study in mice to determine if this response is species specific, and comparison of CO data to “cool white” fluorescent data.

LITERATURE CITED

Chapter One

Adam, D., Dimitrijevic, N., Schartl, M. (1993) Tumor Suppression in Xiphophorus by an Accidentally Acquired Promoter. Science. 259(5096): 816-819.

Ahmed, F.E., & Setlow, R.B. (1993) Ultraviolet Radiation-induced DNA Damage and Its Photorepair in the Skin of the Platyfish Xiphophorus. Can. Res. 53: 2249-2255.

Amores, A., Catchen, J., Nanda, I., Warren, W., Walter, R., Schartl, M., Postlethwait, J.H. (2014) A RAD-Tag Genetic Map for the Platyfish (Xiphophorus maculatus) Reveals Mechanisms for Karyotype Evolution Among Teleost Fish. Gen. 197: 625-641.

Anders, F. (1967) Tumour Formation in Platyfish-Swordtail Hybrids as a Problem of Gene Regulation. Expern. 23(1): 1-80.

Anders, F. (1991) Contributions of the Gordon-Kosswig melanoma system to the present concept of neoplasia. Pigment. Cell Res. 3:7-29.

Aparicio, S., Chapman, J., Stupka, E., Putnam, N., Chia, J., Dehal, P., Christoffels, A., Rash, S., Hoon, S., Smit, A., Gelpke, M.D.S., Roach, J., Oh, T., Ho, I.Y., Wong, M., Detter, C., Verhoef, F., Predki, P., Tay, A., Lucas, S., Richardson, P., Smith, S.F., Clark, M.S., Edwards, Y.J.K., Doggett, N., Zharkik, A., Tavtigian, S.V., Pruss, D., Barnstead, M., Evans, C., Baden, H., powell, J., Glusman, G., Rowen, L., Hood, L., Tan, Y.H., Elgar, G., Hawkins, T., Venkatesh, B., Rokhsar, D., Brenner, S. (2002) Whole-Genome Shotgun Assembly and Analysis of the Genome of Fugu rubripes. Science. 297(5585): 1301-1310.

Armstrong, B.K., Kricker, A., English, D.R. (1997) Sun exposure and skin cancer. Aust. J. Derma. 38(1): S1-S6.

Armstrong, T.N., Reimschuessel, R., Bradley, B.P. (2002) DNA damage, histological changes and DNA repair in larval Japanese medaka (Oryzias latipes) exposed to ultraviolet-B radiation. Aquat. Toxicol. 58(1-2): 1-14.

Aruoma, O.I. (1999) Free Radicals, Oxidative Stress, and Antioxidants in Human Health and Disease. JAOCS. 75(2): 199-211.

Benjamin, C.L., & Ananthaswamy, H.N. (2007) p53 and the pathogenesis of skin cancer. Toxic. App. Pharm. 224: 241-248.

Bielski, R.J., Mayor, J., & Rice, J. (1992) Phototherapy With Broad Spectrum White Fluorescent Light: A Comparative Study. Psych. Res. 43: 167-175.

Bofelli, D., Nobrega, M.A., Rubin, E.M. (2004) Comparative Genomics at the Vertebrate Extremes. Nat. Rev. 5: 456-465.

Boveris, A., & Chance, B. (1973) The Mitochondrial Generation of Hydrogen Peroxide. Biochem. J. 134: 707-716.

Chance, R. E. (1983) The effects of two ranges of fluorescent lighting spectra on human physical performance. Dissertation Abstracts International, 43, 2862B. (University Microfilms No. DA8302215).

Chaves, I., Pokorny, R., Byrdin, M., Hoang, N., Ritz, T., Brettel, K. (2011) The Cryptochromes: Blue Light Photoreceptors in Plants and Animals. Annu. Rev. Plant Biol. 62: 335-364.

Damian, D.L., Matthews, Y.J., Phan, T.A., Halliday, G.M. (2011) An action spectrum for ultraviolet radiation-induced immunosuppression in humans. Brit. J. Derma. 164: 657-659.

Diogo, R., Abdala, V., Lonergan, N., Wood, B.A. (2008) From fish to modern humans-comparative anatomy, homologies and evolution of the head and neck musculature. J. Anat. 213: 391-424.

Gilbert, S.F. (2000) Early Development in Fish. In: Developmental Biology. 6th ed. Sunderland (MA): Sinauer Associates. Available from: http://www.ncbi.nlm.nih.gov/books/NBK10100/

Gordon, M. (1927) The Genetics of a Viviparous Top-Minnow Platypoecilus; the Inheritance of Two Kinds of Melanophores. Genetics. 12: 253-278.

Gordon, M. (1931) Hereditary Basis of Melanosis in Hybrid Fishes. Am. J. Can. 15(732): 1495-1523.

Griggsm H.G. & Bender, M.A. (1972) Ultaviolet and Gamma-Ray Induced Reproductive Death and Photoreactivation in a Xenopus Tissue Culture Cell Line. Photochem. Photobio. 15: 517-526.

Hart, R.W., Setlow, R.B., & Woodhead, A.D. (1977) Evidence that pyrimidine dimers in DNA can give rise to tumors. Proc. Natl. Acad. Sci. USA. 74(12): 5574-5578.

Hedges, S.B., & Kumar, S. (2002) Vertebrate Genomes Compared. Science. 297(5585): 1283-1285.

International Human Genome Sequencing Consortium. (2001) Initial sequencing and analysis of the human genome. Nature. 409: 860-921.

Jemal, A., Siegel, R., Ward, E., Murray, T., Xu, J., Smigal, C., Thun, M.J. (2006) Cancer Statistics, 2006. CA. Can. J. Clin. 56: 106-130.

Kallman, K.D. (2001) How the Xiphophorus Problem Arrived in San Marcos, Texas. Mar. Biotechnol. 3. S6-S16. doi: 10.1007/s10126-001-0022-5.

Kazianis, S. Gimenez-Conti, I., Trono, D., Pedroza, A., Chovanec, L.B., Morizot, D.C., Nairn, R.S., Walter, R.B. (2001)a Genetic Analysis of Neoplasia Induced by N-Nitroso-N-methylureas in Xiphophorus Hybrid Fish. Mar. Biotechnol. 3. S37-S43. doi: 10.1007/s10126001-0025-2.

Kazianis, S., Gimenez-Conti, I., Setlow, R.B., Woodhead, A.D., Harshbarger, J.C., Trono, D., Ledesma, M., Nairn, R.S., Walter, R.W. (2001)b MNU Induction of Neoplasia in a Platyfish Model. Lab. Invest. 81(9): 1191-1198.

Kelner, A. (1948) Effect of Visible Light on the Recovery of Streptomyces Griseus Conidia from Ultra-violet Irradiation Injury. Proc. Natl. Acad. Sci. USA. 35(2): 73-79.

Krishan, D. & Painter, R.B. (1973) Photoreactivation and repair replication in rat kangaroo cells. Mut. Res./Fund. Molec. Mech. Muta. 17(2): 213-222.

Kuller, R., & Lindsten, C. (1992) Health and behavior of children in classrooms with and without windows. J. Environ. Psych. 12: 305-317.

Li, J., Liu, Z., Tan, C., Guo, X., Wang, L., Sancar, A., Zhong, D. (2010) Dynamics and mechanism of repair of ultraviolet-induced (6-4) photoproduct by photolyase. Nature. 466: 887-891.

Liu-Smith, F., Dellinger, R., Meyskens Jr., F.L. (2014) Updates of reactive oxygen species in melanoma etiology and progression. Arch. Biochem. Biophys. 563: 51-55.

Ley, R.D. (1985) Photoreactivation of UV-induced pyrimidine dimers and erythema in the marsupial Monodelphis domestica. Proc. Natl. Acad. Sci. USA. 82: 2409-2411.

Loschen, G., & Flohé, L. (1971) Respiratory Chain Linked H2O Production in Pigeon Heart Mitochondria. FEBS Letters. 18(2): 261-264.

Lucero-Vera, A.A., Diederiks, E.M.A., Lashina, T. (2009) Sunny-Cloudy Scale for Setting Color Temperature of White Lights. United States Patent: 12/092,292. Oct. 1st, 2009.

Lund, L.P., Timmins, G.S. (2007) Melanoma, long wavelength ultraviolet and sunscreens: Controversies and potential resolutions. Pharm. Therap. 114: 198-207.

Maverakis, E., Miyamura, Y., Bowen, M.P., Correa, G., Ono, Y., Goodarzi, H. (2010) Light, Including Ultraviolet. J. Autoimmun. 34(3): J247-J257.

Meador, J.A., Walter, R.B., & Mitchell, D.L. (2000) Induction, Distribution and Repair of UV Photodamage in the Platyfish, Xiphophorus signum. Photochem. Photobiol. 72(2): 260-266.

Meierjohann, S., Schartl, M. (2006). From Mendelian to molecular genetics: the Xiphophorus melanoma model. Trend. Gen. 22(12): 655-661.

Meyer, F., Spanner, H.J., Germer, E. (1939). "Metal Vapor Lamp". United States Patent: 2,182,732. Dec. 5th, 1939.

Mitchell, D., & Nairn, R.S. (1989) The Biology of the (6-4) Photoproduct. Photochem. Photobio. 49(6): 805-819.

Mitchell, D.L., Meador, J.A., Byrom, M., Walter, R.B. (2001) Resolution of UV-Induced DNA Damage in Xiphophorus Fishes. Mar. Biotechnol. 3: S61-S71.

Mitchell, D., Paniker, L., Sanchez, G., Trono, D., Nairn, R. (2007) The Etiology of Sunlight-Induced Melanoma in Xiphophorus Hybrid Fish. Molec. Carcin. 46: 679-684.

Mitchell, D.L., Fernandez, A.A., Nairn, R.S., Garcia, R., Paniker, L., Trono, D., Thames, H.D., Gimenez-Conti, I. (2010) Ultraviolet A does not induce melanomas in a Xiphophorus hybrid fish model. Proc. Natl. Acad. Sci. USA. 107(2). 9329-9334.

Nairn, R.S., Kazianis, S., McEntire, B.B., Coletta, L.D., Walter, R.B., Morizot, D.C. (1996). A CDKN2-like polymorphism in Xiphophorus LG V is associated with UV-B-induced melanoma formation in platyfish-swordtail hybrids. Proc. Natl. Acad. Sci. USA. 93. 13042-13047.

Patton, E.E, Mitchell, D.L., Nairn, R.S. (2010) Genetic and environmental melanoma models in fish. Pig. Cell Mel. Res. 23: 314-337.

Poiley, S.M. (1975) Evaluation of Requirements for Defined Laboratory Animals in Biomedical Research. Adv. Pharmacol. Chemother. 12(0): 125-184.

Rastogi, R.P., Richa, Kumar, A., Tyagi, M.B., Sinha, R.P. (2010) Molecular Mechanisms of Ultraviolet Radiation-Induced DNA Damage and Repair. J. Nuc. Acids. doi:10.4061/2010/592980

Russell, W.L. (1941) Inbred and Hybrid Animals and Their Value in Research. 325-348. In: Biology of the Laboratory Mouse. eds. Snell, G.D. The Blakiston Company. Philadelphia. 497.

Sancar, A. (2003) Structure and Function of DNA Photolyase and Cryptochrome Blue-Light Photoreceptors. ACS: Chem. Rev. 103(6): 2203-2237.

Schartl, A., Malitschek, B., Kazianis, S., Borowsky, R., Schartl, M. (1995) Spontaneous Melanoma Formation in Nonhybrid Xiphophorus. Can. Res. 55: 159-165.

Schartl, M., Walter, R.B., Shen, Y., Garcia, T., Catchen, J., Amores, A., Braasch, I., Chalopin, D., Volff, J., Lesch, K., Bisazza, A., Minx, P., Hillier, L., Wilson, R., Fuerstenberg, S., Boore, J., Searle, S., Postlethwait, J.H., Warren, W.C. (2013) The genome of the platyfish Xiphophorus maculatus, provides insights into evolutionary adaptation and several complex traits. Nat. Gen. 45(5): 567-574.

Setlow, R.B., Woodhead, A.D., & Grist, E. (1989) Animal model for ultraviolet radiation-induced melanoma: Platyfish-swordtail hybrid. Proc. Natl. Acad. Sci. USA. 86: 8922-8926.

Setlow, R.B., Grist, E., Thompson, K., Woodhead, A.D. (1993) Wavelengths effective in induction of malignant melanoma. Proc. Natl. Acad. Sci. USA. 90: 6666-6670.

Sheehan, D. (2009) Spectroscopic Techniques. 53-112. In: Physical Biochemistry. 2nd ed. eds. Carden, C., Woods, F. Wiley-Blackwell. West Sussex, UK. 387.

Smets, B.M.J. (1987) Phosphors Based on Rare-Earths, A New Era in Fluorescent Lighting. Mat. Chem. Phys. 16: 283-299.

Srivastava, A.M., & Ronda, C.R. (2003) Phosphors. The Electrochem. Soc. Interf.

Svobodová, A. & Vostálová, J. (2010) Solar radiation induced skin damage: Review of protective and preventive options. Int. J. Radiat. Biol. 86(12): 999-1030.

Takeuchi, S., Zhang, W., Wakamatsu, K., Ito, S., Hearing, V.J., Kraemer, K.H., Brash, D.E. (2004) Melanin acts as a potent UVB photosensitizer to cause an atypical mode of cell death in murine skin. Proc. Natl. Acad. Sci. USA. 101(42): 15076-15081.

Tewari, A., Sarkany, R.P., & Young, A.R. (2012) UVA1 Induces Cyclobutane Pyrimidine Dimers but Not 6-4 photoproducts in Human Skin In Vivo. J. Invest. Derma. 132: 394-400.

Thornton, W.A. (1971) Luminosity and Color-Rendering Capability of White Light. J. Opt. Soc. Amer. 61(9): 1155-1163.

Uchida, N., Mitani, H., Todo, T., Ikenaga, M., Shima, A. (1997) Photoreactivating Enzyme for (6-4) Photoproducts in Cultured Goldfish Cells. Photochem. Photobio. 65(6): 964-968.

Vielkind, U. (1976) Genetic Control of Cell Differentiation in Platyfish-Swordtail Melanomas. J. Exp. Zool. 196: 197-204.

Vielkind, J. & Vielkind, U. (1982) Melanoma Formation in Fish of the Genus Xiphophorus: A Genetically-Based Disorder in the Determination and Differentiation of a Specific Pigment Cell. Can. J. Gen. Cyt. 24(2): 133-149.

Vielkind, J.R., Kallman, K.D. & Morizot, D.C. (1989) Genetics of Melanomas in Xiphophorus Fishes. J. Aquat. Anim. Health 1: 69-77.

Volff, J. (2005) Genome evolution and biodiversity in teleost fish. Heredity. 94: 280-294.

Walter, R.B. & Kazianis, S. (2001) Xiphophorus Interspecies Hybrids as Genetic Models of Induced Neoplasia. ILAR J. 42(4). 299-321.

Weis, S., & Schartl, M. (1998) The Macromelanophore Locus and the Melanoma Oncogenes Xmrk Are Separate Genetic Entities in the Genome of Xiphophorus. Gene. 149: 1909-1920.

Wenk, J., Brenneisen, P., Meewes, C., Wlaschek, M., Peters, T., Blaudschun, R., Ma, W., Kuhr, L., Schneider, L., Scharffetter-Kochanek, K. (2001) UV-Induced Oxidative Stress and Photoaging. Curr. Probl. Dermatol. 29: 83-94.

Wood, S.R., Berwick, M., Lev, R.D., Walter, R.B., Setlow, R.B., Timmins, G.S. (2006) UV causation of melanoma in Xiphophorus is dominated by melanin photosensitized oxidant production. Proc. Natl. Acad. Sci. USA. 103(11): 4111-4115.

Woolfe, A., Goodson, M., Goode, D.K., Snell, P., McEwen, G.K., Vavouri, T., Smith, S.F., North, P., Callaway, H., Kelly, K., Walter, K., Abnizova, I., Gilks, W., Edwards, Y.J.K., Cooke, J.E., Elgar, G. (2005) Highly Conserved Non-Coding Sequences Are Associated with Vertebrate Development. PLOS Bio. 3(1): 0116-0130. doi: 10.1371/journal.pbio.0030007.

Yang, K., Boswell, M., Walter, D.J., Downs, K.D., Gaston-Pravia, K., Garcia, T., Shen, Y., Mitchell, D. L., Walter, R.B. (2014) UVB-induced gene expression in the skin of Xiphophorus maculatus Jp 163 B. Comp. Biochem. Phys. C. 163: 86-94.

Zhang, X., Rosenstein, B.S., Wang, Y., Lebwohl, M., Mitchell, D.M., Wei, H. (1997)a Induction of 8-Oxo-7,8-Dihydro-2'-Deoxyguanosine by Ultraviolet Radiation in Calf Thymus DNA and HeLa Cells. Photochem. Photobio. 65(1): 119-124.

Zhang, X., Rosenstein, B.S., Wang, Y., Lebwhol, M., Wei, H. (1997)b Identification of Possible Reactive Oxygen Species Involved in Ultraviolet Radiation-Induced Oxidative DNA Damage. Free Rad. Bio. Med. 23(7): 980-985.

Chapter Two

Altschul, S.F., Gish, W., Miller, W., Myers, E.W., Lipman, D.J., 1990. Basic local alignment search tool. J. of Mole. Bio. 215, 403-410.

Anders, S., Huber, W., 2010. Differential expression analysis for sequence count data. Genome Biology. 11: R106.

Bartek, J., Lukas, C., Lukas, J. (2004) Checking on DNA Damage in S Phase. Nat. Revs. 5: 792-804.

Bauer, S., Grossmann, S., Vingron, M., Robinson, P.N., 2008. Ontologizer 2.0--a multifunctional tool for GO term enrichment analysis and data exploration. Bioinformatics (Oxford, England) 24, 1650-1651.

Garcia, T.I., Shen, Y., Crawford, D., Oleksiak, M.F., Whitehead, A., Walter, R.B., 2012. RNA-Seq reveals complex genetic response to Deepwater Horizon oil release in Fundulus grandis. BMC genomics. 13, 474.

Geiss, G.K., Bumgarner, R.E., Birditt, B., Dahl, T., Dowidar, N., Dunaway, D.L., Fell, H.P. Ferree, S., George, R.D., Grogan, T., James, J.J., Maysuria, M., Mitton, J.D., Oliveri, P., Osborn, J.L., Peng, T., Ratcliffe, A.L., Webster, P.J., Davidson, E.H., Hood, L., Dimitrov, K. (2008) Direct multiplexed measurement of gene expression with color-coded probe pairs. Nat Biotech. 26: 317-325. doi:10.1038/nbt1385.

Langmead, B., Salzberg, S.L., 2012. Fast gapped-read alignment with Bowtie 2. Nat Meth. 9, 357-359.

Magoc, T., Salzberg, S.L., 2011. FLASH: fast length adjustment of short reads to improve genome assemblies. Bioinformatics (Oxford, England) 27, 2957-2963.

Savage, R., Cooke, E., Darkins, R., Xu, Y., 2011. BHC: Bayesian Hierarchical Clustering. R package version 1.12.0.

Schmittgen, TD., Livak, KJ., 2008. Analyzing real-time PCR data by the comparative CT method. Nat. Protocols. 3, 1101-1108.

Warde-Farley, D., Donaldson, S.L., Comes, O., Zuberi, K., Badrawi, R., Chao, P., Franz, M., Grouios, C., Kazi, F., Lopes, C.T., Maitland, A., Mostafavi, S., Montojo, J., Shao, Q., Wright, G., Bader, G.D., Morris, Q., 2010. The GeneMANIA prediction server: biological network integration for gene prioritization and predicting gene function. Nucleic Acids Res 38, W214-220.

Chapter Three

Benloucif, S., Masana, M.I., Dubocovich, M.L. (1996) Light-induced phase shifts of circadian activity rhythms and immediate early gene expression in the suprachiasmatic nucleus are attenuated in old C3H/HeN mice. Brain Res. 747: 34-42.

Czeisler, C.A., Shanahan, T.L., Klerman, E.B., Martens, H., Brotman, D.J., Emens, J.S., Klein, T., Rizzo III, J.F. (1995) Suppression of Melationin Secretion in Some Blind Patients by Exposure to Bright Light. NE J. Med. 332(1): 6-11.

Ershler, W.B. & Keller, E.T. (2000) Age-Associated Increased Interleukin-6 Gene Expression, Late-Life Diseases, and Frailty. Annu. Rev. Med. 51: 245-270.

Li, Y., Li, G., Wang, H., Du, J., Yan, J. (2013) Analysis of a Gene Regulatory Cascade Mediating Circadian Rhythm in Zebrafish. PLOS Comp. Biol. 9(2): e1002940.

López-Maury, L., Margueratm S., Bähler, J. (2008) Tuning gene expression to changing environments: from rapid responses to evolutionary adaptations. Nat. Revs. Gen. 9: 583-593.

Maverakis, E., Miyamura, Y., Bowen, M.P., Correa, G., Ono, Y., Goodarzi, H. (2010) Light, Including Ultraviolet. J. Autoimmun. 34(3): J247-J257.

Myers, M.P., Wager-Smith, K., Rothenfluh-Hilfiker, A., Young, M.W. (1996) Light-Induced Degradation of TIMELESS and Entrainment of the Drosophilia Circadian Clock. Science. 271(5256): 1736-1740.

Chapter Four:

Abifadel, M., Varret, M., Rabés, J., Allard, D., Ouguerram, K., Devillers, M., Cruaud, C., Benjannet, S., Wickham, L., Erlich, D., Derré, A., Villéger, L., Farnier, M., Beucler, I., Bruckert, E., Chambaz, J., Chanu, B., Lecerf, J., Luc, G., Moulin, P., Weissenbach, J., Prat, A., Krempf, M., Junien, C., Seidah, N., Boileau, C. (2003) Mutations in PCSK9 cause autosomal dominant hypercholesterolemia. Nature Genetics. 34: 154-156.

Andrews, P.D., Knatko, E., Moore, W.J., Swedlow, J.R. (2003) Mitotic mechanics: the auroras come into view. Curr. Opin. Cell Bio. 15: 672-683.

Archambault, V. & Glover, D.M. (2009) Polo-like kinases: conservation and divergence in their functions and regulation. Molec. Cell. Biol. 10: 265-275.

Arjona, A., Boyadjieva, N., Sarkar, D.K. (2004) Circadian Rhythms of Granzyme B, Perforin, IFN-γ, and NK Cell Cytolytic Activity in the Spleen: Effects of Chronic Ethanol. J. Immun. 172(5): 2811-2817.

Bachmann, M. & Möröy, T. (2005) The serine/threonine kinase Pim-1. Int. J. Biochem. Cell. Bio. 37: 726-730.

Baker, J. & Garrod, D. (1993) Epithelial cells retain junctions during mitosis. J. Cell. Sci. 104: 415-425.

Bang, M., Centner, T., Fornorr, F., Geach, A.J., Gotthardt, M., McNabb, M., Witt, C.C., Labeit, D., Gregorio, C.C., Granzier, H., Labeit, S. (2001) The Complete Gene Sequence of Titin, Expression of an Unusual ≈700-kDa Titin Isoform, and Its Interaction With Obscurin Identity a Novel Z-Line to I-Band Linking System. Circ. Res. 89: 1065-1072.

Barbieri, E., de Preter, K., Capasso, M., Chen, Z., Hsu, D.M., Tonini, G.P., Lefever, S., Hicks, J., Versteeg, R., Pession, A., Speleman, F., Kim, E.S., Shohet. (2013) Histone Chaperone CHAF1A Inhibits Differentiation and Promotes Aggressive Neuroblastoma. Cancer Res. 74(3): 765-774.

Bartek, J., Lukas, C., Lukas, J. (2004) Checking on DNA Damage in S Phase. Nat. Revs. 5: 792-804.

Bayliss, R., Sardon, T., Vernos, I., Conti, E. (2003) Structural Basis of Aurora-A Activation by TPX2 at the Mitotic Spindle. Molec. Cell. 12: 851-862.

Bennet, V. (1990) Spectrin: a structural mediator between diverse plasma membrane proteins and the cytoplasm. Curr. Opin. Cell Bio. 2:51-56.

Blind, R.D., Suzawa, M., Ingraham, H.A. (2012) Direct modification and regulation of nuclear receptor-PIP2 complex by the nuclear inositol-lipid kinase IPMK. Sci. Signal. 5(229): ra44.

Bornslaeger, E.A., Corcoran, C.M., Stappenback, T.S., Green, K.J. (1996) Breaking the Connection: Displacement of the Desmosomal Plaque Protein Desmoplakin from Cell-Cell Interfaces Disrupts Anchorage of Intermediate Filament Bundles and Alters Intercellular Junction Assembly. J. Cell Bio. 134(4): 985-1001.

Bradley, W.D. & Koleske, A.J. (2009) Regulation of cell migration and morphogenesis by Abl-family kinases: emerging mechanisms and physiological contexts. J. Cell. Sci. 122(19): 3441-3454.

Bruce, C., Hoy, A.J., Turner, N., Watt, M.J., Allen, T.L., Carpenter, K., Cooney, G.J., Febbraio, M.A., Kraegen, E.W. (2009) Overexpression of Carnitine Palmitoyltransferase-1 in Skeletal Muscle Is Sufficient to Enhance Fatty Acid Oxidation and Improve High-Fat Diet-Induced Insulin Resistance. Diabetes. 58: 550-558.

Cahill, M.E., Xie, Z., Day, M., Photowala, H., Barbolina, M.V., Miller, C.A., Weiss, C., Radulovic, J., Sweatt, D., Disterhoft, J.F., Surmeier, D.J., Penzes, P. (2009) Kalirin regulates cortical spine morphogenesis and disease-related behavioral phenotypes. PNAS. 106(31): 13058-13063.

Casanova, C.M., Rybina, S., Yokoyama, H., Karsenti, E., Mattaj, I.W. (2008) Hepatoma Up-Regulated Protein is Required for Chromatin-induced Microtubule Assembly Independetly of TPX2. Mol. Biol. Cell. 19(11): 4900-4908.

Champliaud, M., Baden, H., Koch, M., Jin, W., Burgeson, R.E., Viel, A. (2000) Gene Characterization of Sciellin (SCEL) and Protein Localization in Vertebrate Epithelia Displaying Barrier Properties. Genomics. 70: 264-268.

Cho, W., Lee, Y., Kong, S., Hurwitz, J., Lee, J. (2006) CDC7 kinase phosphorylates serine residues adjacent to acidic amino acids in the minichromosome maintenance 2 protein. PNAS. USA. 103(31): 11521-11526.

Choi, B., Pagano, M., Dai, W. (2014) Plk1 Protein Phosphorylates Phosphatase and Tensin Homolog (PTEN) and Regulates Its Mitotic Activity during the Cell Cycle. J. Bio. Chem. 289(20): 14066-14074.

Crowley, J. L., Smith, T. C., Fang, Z., Takizawa, N., & Luna, E. J. (2009) Supervillin Reorganizes the Actin Cytoskeleton and Increases Invadopodial Efficiency. Molecular Biology of the Cell, 20(3), 948–962. doi:10.1091/mbc.E08-08-0867.

Davenport, J.W., Fernandes, E.R., Harris, L.D., Neale, G.A.M., Goorha, R. (1998) Genomics. 55: 113-117.

Ditchfield, C., Johnson, V.L., Tighe, A., Ellston, R., Haworth, C., Johnson, T., Mortlock, A., Keen, N., Taylor, S.S. (2003) Aurora B couples chromosome alignment with anaphase by targeting BubR1, Mad2, and Cenp-E to kinetochores. J. Cell. Bio. 161(2): 267-280.

Dephoure, N., Zhou, C., Villén, J., Beausoleil, S.A., Bakalarski, C.E., Elledge, S.J., Gygi, S.P. (2008) A quantitative atlas of mitotic phosphorylation. PNAS. 105(31): 10762-10767.

Doi, M., Okano, T., Yujnovsky, I., Sassone-Corsi, P., Fukada, Y. (2004) Negative Control of Circadian Clock Regulator E4BP4 by Casein Kinase Iε-Mediated Phosphorylation. Curr. Bio. 14: 975-980.

Dorée, M. and Galas, S. (1994) The cyclin-dependent protein kinases and the control of the cell division. FASEB J. 8: 1114-1121.

Doublié, S., Bricogne, G., Gilmore, C., Carter, C.W. Jr. (1995) Tryptophanyl-tRNA synthetase crystal structure reveals an unexpected homology to tyrosyl-tRNA synthetase. Structure. 3:17-31.

Dupont, E., Gomez, J., Bioldeau, D. (2013) Beyond UV radiation: A skin under challenge. Int. J. Cos. Sci. 35: 224-232.

Eckel, R.H. (1989) Lipoprotein lipase. A multifunctional enzyme relevant to common metabolic diseases. N. Eng. J. Med. 320(16): 1060-1068.

Eckert, R.L., Sturniolo, M.T., Broome, A., Ruse, M., Rorke, E.A. (2005) Transglutaminase Function in Epidermis. J. Invest. Dermatol. 124: 481-492.

Eming, S.A., Krieg, T., Davidson, J.M. (2007) Inflammation in Wound Repair: Molecular and Cellular Mechanisms. J. Invest. Derm. 127: 514-525.

Falvey, E., Olela, F., Schibler, U. (1995) The rat hepatic leukemia factor (hlf) gene encodes two transcriptional activators with distinct circadian rhythms, tissue distributions and target preferences. EMBO. J. 14(17): 4307-4317.

Feuerborn, A., Srivastava, P.K., Küffer, S., Grandy, W.A., Sijmonsma, T.P., Gretz, N., Brors, B., Gröne, H.J. (2011) The Forkhead Factor FoxQ1 Influences Epithelial Differentiation. J. Cell. Physiol. 226: 710-719.

Fish, J.L., Kosodo, Y., Enard, W., Pääbo, S., Huttner, W.B. (2006) Aspm specifically maintains symmetric proliferative divisions of neuroepithelial cells. PNAS. 103(27): 10438-10443.

Flaxman, B.A. 7 Chopra, D.P. (1972) Cell Cycle of Normal and Psoriatic Epidermis in vitro. J. Invest. Derm. 59(1): 102-105.

Fleischmajer, R., Utani, A., MacDonald, E.D., Parlish, J.S., Pan, T., Chu, M., Nomizu, M., Ninomiya, Y., Yamada, Y. (1998) Initiation of skin basement membrane formation at the epidermo-dermal interface involves assembly of laminins through binding to cell membrane receptors. J. Cell Sci. 111: 1929-1940.

Flydal, M.I. & Martinez, A. (2013) Phenylalanine Hydroxylase: Function, Structure, and Regulation. IUBMB. 65(4): 341-349.

Fontaine, C., Dubois, G., Duguay, Y., Helledie, T., Vu-Dac, N., Gervois, P., Soncin, R., Mandrup, S., Fruchat, J.C., Fruchart-Najib, J., Staels, B. (2003) "The orphan nuclear receptor (PPAR) gamma target gene and promotes PPARgamma-induced adipocyte differentiation". J. Biol. Chem. 278: 37672-37680.

Francone, V.P., Ifrim, M.F., Rajagopal, C., Leddy, C.J., Wang, Y., Carson, J.H., Mains, R.E., Eipper, B.A. (2010) Signaling from the Secretory Granule to the Nucleus: Uhmk1 and PAM. Molec. Endocrin. 24: 1543-1558.

Frisch, S.M. & Francis, H. (1994) Disruption of Epithelial Cell-Matrix Interactions Induces Apoptosis. J. Cell. Bio. 124(4): 619-626.

Gant, R., Parshad, R., Ewig, R.A.G., Sanford, K.K., Jones, G.M., Tarone, R.E., Kohn, K.W. (1978) Fluorescent light-induced DNA crosslinkage and chromatid breaks in mouse cells in culture. PNAS. USA. 75(8): 3809-3812.

Gaudet, S., Branton, D., Lue, R.A. (2000) Characterization of PDZ-binding kinase, a mitotic kinase. PNAS. 97(10): 5167-5172.

Geiman, T.M., Durum, S.K., Muegge, K. (1998) Characterization of Gene Expression, Genomix Structure, and Chromosomal Localization of Hells (Lsh). Genomics. 54: 477-483.

Glasauer, S.M.K & Neuhauss, S.C.F. (2014) Whole-genome duplication in teleost dishes and its evolutionary consequences. Mol. Genet. Genomics. 289: 1045-1060.

Golsteyn, R.M., Mundt, K.E., Fry, A.M., Nigg, E.A. (1995) Cell Cycle Regulation of the Activity and Subcellular Localization of PLK1, a Human Protein Kinase Implicated in Mitotic Spindle Formation. J. Cell. Bio. 129(6): 1617-1628.

Grossman, J. (2002) Molecular mechanisms of "detachment-induced apoptosis-Anoikis". Apoptosis. 7: 247-260.

Gumbiner, B.M. (1996) Cell Adhesion: The Molecular Basis of Tissue Architecture and Morphogenesis. Cell. 84: 345-357.

Hartwell, L.H. & Kastan, M.B. (1994) Cell Cycle Control and Cancer. Science. 266(5192): 1821-1828.

Haring, S.J., Mason, A.C., Binz, S.K., Wold, M.S. (2008) Cellular Functions of Human RPA1. J. Bio. Chem. 283(27): 19095-19111.

Hirokawa, N. & Takemura, R. (2004) Kinesin superfamily proteins and their various functions and dynamics. Exp. Cell Res. 301: 50-59.

Hirose, K., Kawashima, T., Iwamoto, I., Nosaka, T., Kitmura, T. (2001) MgcRacGAP Is Involved in Cytokinesis through Associating with Mitotic Spindle and Midbody. J. Biol. Chem. 276: 5821-5828.

Hui, S.T.Y., Andres, A.M., Miller, A.K., Nathanael, J.S., Potter, D.W., Post, N.M., Chen, A.Z., Sachithanantham, S., Jung, D., Kim, J.K., Davis, R.A. (2008) Txnip balances metabolic and growth signaling via PTEN disulfide reduction. PNAS. 105(10): 3921-3926.

Hung, L., Tang, C., Tang, T. (2000) Protein 4.1 R-135 Interacts with a novel Centrosomal Protein (CPAP) Which is Associated with the ϒ-Tubulin Complex. Molec. Cell. Bio. 20(20): 7813-7825.

Jain, M., Zhang, L., Boufraqech, M., Liu-Chittenden, Bussey, K., Demeure, M.J., Wu, X., Su, L., Pacak, K., Strtakis, C.A., Kebebew, E. (2014) ZNF367 Inhibits Cancer Progression and Is Targeted by miR-195. PLoS ONE. 9(7):e101423.

Jais, A., Matori, M., Kittakoop, P., Sowanborirux, K. (1998) Fatty Acid Compositions in Mucus and Roe of Haruan, Channa Striatus, for Wound Healing. Gen. Pharmac. 30(4): 561-563.

Karashima, T. & Watt, F.M. (2002) Interaction of periplakin and envoplakin with intermediate filaments. J. Cell Sci. 115(24): 5027-5037.

Kikuchi, G., Motokawa, Y., Yoshida, T., Hiraga, K. (2008) Glycine cleavage system: reaction mechanism, physiological significance, and hyperglycemia. Proc. Jpn. Acad., Ser. B. 84: 246-263.

Kitano-Takahashi, M., Morita, H., Kondo, S., Tomizawa, K., Kato, R., Tanio, M., Shirota, Y., Takahashi, H., Sugio, S., Kohno, T. (2007) Expression, purification and crystallization of a human tau-tubulin kinase 2 that phosphorylates tau protein. Acta. Cryst. F63: 602-604.

Kobayashi, Y., Ishikawa, T., Hirayama, J., Daiyasu, H., Kanai, S., toh, H., Fukuda, I., Tsujimura, T., Terada, N., Kamei, Y., Yuba, S., Iwai, S., Todo, T. (2000) Molecular analysis of zebrafish photolyase/cryptochrome family: two types of cryptochromes present in zebrafish. Genes. Cells. 5: 725-738.

Lammens, T., Li, J., Leone, G., De Veylder, L. (2009) Atypical E2Fs: new players in the E2F transcription factor family. Trends Cell Bio. 19(3): 111-118.

Lauriola, M., Enuka, Y., Zeisel, A., D'Uva, G., Roth, L., Sharon-Sevilla, M., Lindzen, M., Sharma, K., Nevo, N., Feldman, M., Carvalho, S., Cohen-Dvashi, H., Kedmi, M., Ben-Chetrit, N., Chen, A., Solmi, R., Weimann, S., Schmitt, F., Domany, E., Yarden, Y. (2014) Diurnal suppression of EGFR signaling by glucocorticoids and implications for tumour progression and treatment. Nat. Comm. 5(5073). doi: 10.1038/ncomms6073.

Lee, W.H., Lukacik, P., Guo, K., Ugochukwu, E., Kavanagh, K.L., Marsden, B., Oppermann, U. (2009) Structure-activity relationships of human AKR-type oxidoreductases involved in bile acid synthesis: AKR1D1 and AKR1C4. Molec. Cell. Endo. 301: 199-204.

Lei, M. & Tye, B.K. (2001) Initiating DNA synthesis: from recruiting to activating the MCM complex. J. Cell Sci. 114(8): 1447-1454.

Liao, H., Winkfein, R.J., Mack, G., Rattner, J.B., Yen, T.J. (1995) CENP-F Is a Protein of the Nuclear Matrix That Assembles onto Kinetochores at Late G2 and Is Rapidly Degraded After Mitosis. J. Cell Bio. 130(3): 507-518.

Lidral, A.C., Romitti, P.A., Basart, A.M., Doetschman, T., Leysens, N.J., Daack-Hirsch, S., Semina, E.V., Johnson, L.R., Machida, J., Burds, A., Parnell, T.J., Rubenstein, J.L.R., Murray, J.C. (1998) Association of MSX1 and TGFB3 with Nonsydromic Clefting in Humans. Am. J. Hum. Genet. 63:557-568.

Lin, M. & Khnykin, D. (2014) Fatty acid transporters in skin development, function and disease. Biochim. Biophys. Acta. 1841: 362-368.

Lisby, M., Rothstein, R., Mortensen, U.H. (2001) Rad52 forms DNA repair and recombination centers during S phase. PNAS. 98(15): 8276-8282.

Liu, S., Song, N., Zou, L. (2012) The conserved C terminus of Claspin interacts with Rad9 and promotes rapid activation of Chk1. Cell Cycle. 11(14): 2711-2716.

Machius, M., Chuang, J.L., Wynn, R.M., Tomchick, D.R., Chuang, D.T. (2001) Structure of rat BCKD kinase: Nucleotide-induced domain communication in a mitochondrial protein kinase. PNAS. 98(20): 11218-11223.

Malumbres, M. & Barbacid, M. (2007) Cell cycle kinases in cancer. Curr. Opin. Gen. Develop. 17: 60-65.

Mertelot, G., Claudiel, T., Gatfield, D., Schaad, O., Kornmann, B., Sasso, G., Moschetta, A., Schibler, U. (2009) REV-ERBα Participates in Circadian SREBP Signaling and Bile Acid Homeostasis. PLoS Bio. 7(9): e1000181. doi: 10.1371/journal.pbio.1000181.

Moldovan, G., Pfander, B., Jentsch, S. (2007) PCNA, the Maestro of the Replification Fork. Cell. 129: 665-679.

Moran, G.R. (2005) 4-hydroxyphenylpyruvate dioxygenase. Arch. Biochem. Biophys. 433: 117-128.

Nay, S.L., Lee, D., Bates, S.E., O'Connor, T.R. (2012) Alkbh2 protects against lethiality and mutation in primary mouse embryonic fibroblasts. DNA Repair. 11: 502-510.

Nickoloff, B.J., Qin, J., Chaturvedi, V., Denning, M.F., Bonish, B., Miele, L. (2002) Jagged-1 mediated activation of notch signaling induces complete maturation of human keratinocytes through NF-κB and PPARγ. Cell. Death. Diff. 9:842-855.

Nishtani, H., Lygerou, Z., Nishimoto, T., Nurse, P. (2000) The Cdt1 protein is reuired to license DNA for replication in fission yeast. Nature. 404: 625-628.

Oliveri, P., Fortunato, A.E., Petrone, L., Ishikawa-Fujiwara, T., Kobayashi, Y., Todo, T., Antonova, O., Arboleda, E., Zantke, J., Tessmar-Raible, K., Falciatore, A. (2014) The Cryptochrome/Photolyase Family in aquatic organisms. Marine Genomics. 14: 23-37.

Park, S.T., Aldape, R.A., Futer, O., DeCenzo, M.T., Linvingston, D.J. (1992) PPIase Catalysis by Human FK506-binding Protein Proceeds Through a Conformational Twist Mechanism. J. Bio. Chem. 267(5): 3316-3324.

Phornphutkul, C., Introne, W.J., Perry, M.B., Bernardini, I., Murphey, M.D., Fitzpatrick, D.L., Anderson, P.D., Huizing, M., Anikster, Y., Gerber, L.H. Gahl, W.A. (2002) Natural History of Alkaptonuria. N. Engl. J. Med. 347(26): 2111-2121.

Praekelt, U., Kopp, P. M., Rehm, K., Linder, S., Bate, N., Patel, B., […] Monkley, S. J. (2012). New isoform-specific monoclonal antibodies reveal different sub-cellular localisations for talin1 and talin2. Euro. J. Cell. Biol. 91(3), 180–191. doi:10.1016/j.ejcb.2011.12.003.

Randall, D.J. & Wright, P.A. (1987) Ammonia distribution and excretion in fish. Fish. Phys. Biochem. 3(3): 107-120.

Reppert, S.M., Weaver, D.R. (2002) Coordination of circadian timing in mammals. Nature. 418: 935-941.

Rhee, S.G. (2001) Regulation of Phosphoinositide-Specific Phospholipase C. Annu. Rev. Biochem. 70: 281-312.

Rose, A.J., Alstedm T.J., Jensen, T.E., Kobbero, Maarbjerg, S.J., Jensen, J., Richter, E.A. (2009) A Ca2+ -calmodulin-eEF2K-eEF2 signaling cascade, but not AMPK, contributes to the suppression of skeletal muscle protein synthesis during contractions. J. Physiol. 587(7): 1547-1563.

Ruiz, X.D., Mlakar, L.R., Yamaguchi, Y., Su, Y., Larregina, A.T., Pilewski, J.M., Feghali-Bostwick, C.A. (2012) Syndecan-2 Is a Novel Target of Insulin-Like Growth Factor Binding Protein-3 and Is Over-Expressed in Fibrosis. PLoS ONE. doi: 10.1371/journal.pone.0043049.

Rurhberg, C. & Watt, F.M. (1997) The plakin family: versatile organizers of cytoskeletal architecture. Curr. Opin. Gen. Dev. 7(3): 392-397.

Schlessinger, J. Cell signaling by receptor tyrosine kinases. Cell. 103: 211-225.

Schneider, L., Essmann, F., Kletke, A., Rio, P., Hanenberg, H., Wetzel, W., Schulze-Osthoff, K., Nürnberg, B., Piekorz, R.P. (2007) The Transforming Acidic Coiled Coil 3 Protein Is Essential for Spindle-dependent Chromosome Alignment and Mitotic Survival. J. Bio. Chem. 282(40): 29273-29283.

Schlozen, T. & Gerdes, J. (2000) The Ki-67 Protein: From the Known and the Unknown. J. Cell. Phys. 182: 311-322.

Scloz, M., Widlund, P.O., Piazza, S., Bublik, D.R., Reber, S., Peche, L.Y., Ciani, Y., Hubner, N., Isokane, M., Monte, M., Ellenberg, J., Hyman, A.A., Scheider, C., Bird, A.W. (2000) GTSE1 Is a Microtubule Plus-End Tracking Protein That Regulates EB1-Dependent Cell Migration. PLoS ONE. 7(12): e51259. doi: 10.1371/journal.pone.0051259.

Sebolt-Leopold, J.S., Dudley, D.T., Herrera, R., van Becelaere, K., Wiland, A., Gowan, R.C., Tecle, H., Barrett, S.D., Bridges, A., Przybranowski, S., Leopold, W.R., Saltiel, A.R. (1999) Blockade of the MAP kinase pathway suppresses growth of colon tumors in vivo. Nat. Med. 5(7): 810-816.

Sekiguchi, T., Mizutani, T., Yamada, K., Kajitani, T., Yazawa, T., Yoshino, M., Miyamoto, K. (2004) Expression of epiregulin and amphiregulin in the rat ovary. J. Molec. Endo. 33: 281-291.

Sekiya, M., Osuga, J., Igarashi, M., Okazaki, H., Ishibashi, S. (2011) The Role of Neutral Cholesterol Ester Hydrolysis in Macrophage Foam Cells. J. Athero. Throm. 18(5): 359-364.

Sherr, C.J. (1993) Mammalian G1 Cyclins. Cell. 73: 1059-1065.

Shirakata, Y., Komurasaki, T., Toyoda, H., Hanakawa, Y., Yamasaki, K., Tokumaru, S., Sayama, K., Hashimoto, K. (2000) Epiregulin, a Novel Member of the epidermal Growth Factor Family, Is an Autocrine Growth factor in Normal Human Keratinocytes. J. Biol. Chem. 275(8): 5478-5753.

Siu, F., Bain, P.J., LeBlanc-Chaffin, R., Chen, H., Kilberg, M.S. (2002) ATF4 Is a Mediator of the Nutrient-sensing Response Pathway That Activates the Human Asparagine Synthetase Gene. J. Bio. Chem. 27(5): 24120-24127.

Song, T., Hatano, N., Horii, M., Tokumitsu, H., Yamaguchi, F., Tokuda, M., Watanabe, Y. (2004) Calcium/calmodulin-dependent protein kinase 1 inhibits neuronal nitric-oxidase synthase activity through serine 741 phosphorylation. FEBS Lett. 570(1-3): 133-137.

Steger, D.J., Lefterova, M.I., Ying, L., Stonestrom, A.J., Schupp, M., Zhuo, D., Vakoc, A.L., Kim, J., Chen, J., Lazar, M.A., Blobel, G.A., Vakoc, C.R. (2008) DOT1L/KMT4 Recruitment and H3K79 Methylation Are Ubiquitously Coupled with Gene Transcription in Mammalian Cells. Mol. Cell Bio. 28(8): 2825-2839.

Swanson, B.J., Jack, H.M. and Lyons, G.E. (1998) Characterization of myocyte enhancer factor 2 (MEF2) expression in B and T cells: MEF2C is a B cell-restricted transcription factor in lymphocytes. Mol. Immunol., 35, 445–458.

Takahashi, J.S., Hong, H., Ko, C.H., McDearmon, E.L. (2008) The genetics of mammalian circadian order and disorder: implications for physiology and disease. Nat. Rev. Gen. 9: 764-775.

Tamai, T.K., Young, L.C., Whitmore, D. (2007) Light signaling to the zebrafish circadian clock by Cryptochrome 1a. PNAS. 104(37): 14712-14717.

Tamai, T.K., Young, L.C., Cox, C.A., Whitmore, D. (2012) Light Acts on the Zebrafish Circadian Clock to Suppress Rhythmic Mitosis and Cell Proliferation. J. Biol. Rhyt. 27(3): 226-236.

Tange, Z., Sun, Y., Harley, S.E., Zou, H., Yu, H. (2004) Human Bub1 protects centromeric sister-chromatid cohesion through Shugoshin during mitosis. PNAS. 101(52): 18012-18017.

Tavakkol, A., Elder, J.T., Griffiths, C.E.M., Cooper, K.D., Talwar, H., Fisher, G.J., Keane, K.M., Foltin, S.K., Voorhees, J.J. (1992) Expression of Growth Hormone Receptor, Insulin-Like Growth Factor 1 (IGF-1) and IGF-1 Receptor mRNA and Proteins in Human Skin. Soc. Invest. Derm. 99: 343-349.

Taylor, S.S. & McKeon, F. (1997) Kinetochore Localization of Murine Bub1 is Required for Normal Mitotic Timing and Checkpoint Response to Spindle Damage. Cell. 89(5): 727-735.

Timpl, R., Rohde, H., Robey, P.G., Rennard, S.I., Foidart, J., Martin, G.R. (1979) Laminin-A Glycoprotein from Basement Membranes. J. Bio. Chem. 254(19): 9933-9937.

Troelstra, C., Hesen, W., Bootsma, D., Hoeijmakers, J.H.J. (1993) Structure and expression of the excision repair gene ERCC6, involved in the human disorder Cockayne's syndrome group B. Nuc. Acid. Res. 21(3): 419-426.

Tsuchida, K., Nakatani, M., Yamakawa, N., Hashimoto, O., Hasegawa, Y., Sugino, H. (2004) Activin isoforms signal through type 1 receptor serine/threonine kinase ALK7. Mole. Cell. Endo. 220(1-2): 59-65.

Uitto, J., Olsen, D., Fazio, M.J. (1989) Extracellular Matrix of the Skin: 50 Years of Progress. J. Invest. Derm. 92(4): 61S-77S.

Vainio, S. & Ikonen, E. (2003) Macrophage cholesterol transport: a critical player in foam cell formation. Annu. Med. 35: 146-155.

Vasioukhni, V., Bauer, C., Yin, M., Fuchs, S. (2000) Directed Actin Polymerization Is the Driving Force for Epithelial Cell-Cell Adhesion. Cell. 100: 209-219.

Vatine, G., Vallone, D., Gothil, Y., Foulkes, N.S. (2011) It's time to swim! Zebrafish and the circadian clock. FEBS Letters. 585(10): 1485-1494.

Vasioukhin, V., Bowers, E., Bauer, C., Degenstein, L., Fuchs, E. (2001) Desmoplakin is essential in epidermal sheet formation. Nat. Cell Bio. 3: 1076-1085.

Virshup, D.M., Eide, E.J., Forger, D.B., Gallego, M., Vielhaber Harnish, E. (2007) Reversible Protein Phosphorylation Regulates Circadian Rhythms. C.S.H Symp. Quant. Bio. 72: 413-420.

Walker, M.G. (2001) Drug Target Discovery by Gene Expression Analysis: Cell Cycle Genes. Curr. Canc. Drug. Targ. 1: 73-83.

Walter, M.G. (2001) Drug Target Discovery by Gene Expression Analysis: Cell Cycle Genes. Curr. Canc. Drug Targ. 1:73-83.

Walter, D.J., Boswell, M., Volk de García, Walter, S.M., Breitenfeldt, E.W., Boswell, W., Walter, R.B. (2014) Characterization and differential expression of CPD and 6-4 DNA photolyases in Xiphophorus species and interspecies hybrids. Comp. Biochem. Phys. C. 163: 77-85.

Weiner, D. & Verlander, J.W. (2014) Ammonia transport in the kidney by Rhesus glycoproteins. Am. J. Physiol. Renal Physiol. 306(10): F1107-F1120.

Wilde, A. (2006) “HURP on” we’re off to the kinetochore!. J. Cell. Bio. 173(6): 829-831.

Wilsbacher, L.D., Takahashi, J.S. (1998) Circadian rhythms: molecular basis of the clock. Curr. Opn. Gen. Develp. 8: 595-602.

Wright, P.A. & Wood, C.M. (2009) A new paradigm for ammonia excretion in aquatic animals: role of Rhesus (Rh) glycoproteins. J. Exp. Bio. 212: 2303-2312.

Xu, Z., Ogawa, H., Vagnarelli, P., Bergmann, J.H., Hudson, D.F., Ruchaud, S., Fukagawa, T., Earnshaw, W.C., Samejima, K. (2009) INCENP-aurora B interactions modulate kinase activity and chromosome passenger complex localization. J. Cell Biol. 187(5): 637-53.

Yang, K., Boswell, M., Walter, D.J., Downs, K.D., Gaston-Pravia, K., Garcia, T., Shen, Y., Mitchell, D. L., Walter, R.B. (2014) "UVB-induced gene expression in the skin of Xiphophorus maculatus Jp 163 B". Comp. Biochem. Phys. C. 163: 86-94.

Yang, D., Feng, S., Chen, W., Zhao, H., Paulson, C., Li, Y. (2012) V-ATPase subunit ATP6AP1 (Ac45) regulates osteoclast differentiation, extracellular acidification, lysosomal trafficking, and protease exocytosis in osteoclast-mediated bone resorption. J. Bone. Min. Res. 27(8): 1695-1707.

Zhang, X., Horwitz, G.A., Prezant, T.R. Valentini, A., Nakashima, M., Bronstein, M.D., Melmed, S. (1999) Structure, Expression, and Function of Human Pituitary Tumor-Transforming Gene (PTTG). Molec. Endocrin. 13(1): 156-166.

Chapter Five

Cooper, G.M. The Cell: A Molecular Approach. 2nd edition. Sunderland (MA): Sinauer Associates; 2000. The Eukaryotic Cell Cycle. Available from: http://www.ncbi.nlm.nih.gov/books/NBK9876.

Esteban, M.A. (2012) An Overview of the Immunological Defenses in Fish Skin. ISRN Immun. ID: 853470. doi: 10.5402/2012/853470.

Flaxman, B.A. 7 Chopra, D.P. (1972) Cell Cycle of Normal and Psoriatic Epidermis in vitro. J. Invest. Derm. 59(1): 102-105.

Foster, D.A., Yellen, P., Xu, L., Saqcena, M. (2011) Regulation of G1 Cell Cycle Progression: Distinguishing the Restriction Point from a Nutrient-Sensing Cell Growth Checkpoint. Genes & Cancer. 1(11): 1124-1131.

Schlozen, T. & Gerdes, J. (2000) The Ki-67 Protein: From the Known and the Unknown. J. Cell. Phys. 182: 311-322.

van Erp, P.E., Boezeman, J.B., Brons, P.P. (1996) Cell cycle kinetics in normal human skin by in vivo administration of iododeoxyuridine and application of a differentiation marker—implications for cell cycle kinetics in psoriatic skin. Anal. Cell. Pathol. 11(1): 43-54.

Xie, Z., Komuves, L., Yu, Q., Elalieh, H., Ng, D.C., Leary, C., Chang, S., Crumrine, D., Yoshizawa, T., Kato, S., Bikle, D.D. (2002) Lack of the Vitamin D Receptor is Associated with Reduced Epidermal Differentiation and Hair Follicle Growth. J. Invest. Derma. 118(1): 11-16.